

Aalto University
School of Engineering
Master's Programme in Building Technology

Henri Kuronen

Tensile strength of wood in high temperatures before charring

Master's Thesis
Espoo, November 5, 2018

Supervisor: Prof. Simo Hostikka
Advisor: Esko Mikkola D.Sc. (Tech.)

Author:	Henri Kuronen		
Title:	Tensile strength of wood in high temperatures before charring		
Date:	November 5, 2018	Pages:	120
Major:	Building Technology	Code:	CIV
Supervisor:	Prof. Simo Hostikka		
Advisor:	Esko Mikkola D.Sc. (Tech.)		
<p>The area under the examination in this thesis is the behaviour of wood in exposure to high temperatures, before charring. The main focus is temperature's effects on tensile strength. This is first done by examining relevant literature and studies, after which the design aspects are analyzed. Next part of the thesis are the tensile strength experiments conducted in high temperatures.</p> <p>The testing method used in this thesis was steady-state test, where the temperature of the sample is kept constant, and the tension is increased until yielding. Samples were manufactured out of spruce.</p> <p>Based on the connection between temperature and tensile strength presented throughout this thesis, an example of a practical application is derived through a small software built for the purpose of this work. This software can be used as a tool in analysing the results of a fire simulation.</p> <p>The main objective of this thesis was to gather knowledge on the effects of the temperature on tensile strength, and evaluate the adequacy of different design approaches on the fire behaviour of wood, explained in the Eurocode 5. This analysis and complementation of the underlying patterns of the fire design of timber was mainly achieved via tensile tests in elevated temperatures. The results of these tensile strength experiments showed that the correlation between temperature and tensile strength presented in the Eurocode can be used as a good approximation in design applications.</p>			
Keywords:	fire safety, timber, tensile strength, elevated temperatures		
Language:	English		

Tekijä:	Henri Kuronen		
Työn nimi:	Puun vetolujuus korkeissa lämpötiloissa ennen hiiltymistä		
Päiväys:	5. marraskuuta 2018	Sivumäärä:	120
Pääaine:	Building Technology	Koodi:	CIV
Valvoja:	Professori Simo Hostikka		
Ohjaaja:	TkT Esko Mikkola		
<p>Tarkastelun kohteena tässä diplomityössä on puun käyttäytyminen altistettuna korkeille lämpötiloille, ennen hiiltymistä. Pääpainona toimii lämpötilan vaikutus vetolujuuteen. Kyseinen tarkastelu suoritetaan ensin kirjallisuuskatsauksen muodossa, jonka jälkeen suunnitteluprosessiin sisältyvät asiat ovat tarkemman analysoinnin kohteena. Diplomityön seuraavassa osassa suoritetaan puun vetokokeet korkealle lämpötilalle altistettuna.</p> <p>Koemenetelmänä käytettiin vakiolämpötilassa suoritettavaa koetta, jossa kappaleeseen kohdistuvaa jännitystä kasvatettiin kappaleen murtumiseen asti. Kokeissa käytetyt näytteet valmistettiin kuusesta.</p> <p>Tässä työssä esiteltiin lämpötilan ja vetolujuuden väliseen yhteyteen perustuen luotiin käytännön sovelluksena pieni ohjelmisto, jota voidaan käyttää apuna palosimulointitulosten analysointiin.</p> <p>Tämän diplomityön päätavoitteena oli kerätä tietoa lämpötilan vaikutuksesta puun vetolujuuteen, sekä arvioida Eurokoodi 5:ssä esiteltyjen suunnitteluperiaatteiden pätevyyttä. Tämä puun palomitoituksen taustalla olevien mallien analysointi sekä täydentäminen saavutettiin pääosin vetokokeilla korotetuissa lämpötiloissa. Näiden vetokokeiden tulosten perusteella voidaan sanoa Eurokoodissa esitellyn lämpötilan ja vetolujuuden yhteyden olevan hyvä approksimaatio suunnittelutarkoituksiin.</p>			
Asiasanat:	paloturvallisuus, puu, vetolujuus, kohotettu lämpötila		
Kieli:	Englanti		

Forewords

I would like to thank my thesis supervisor Professor Simo Hostikka and advisor D.Sc. (Tech.) Esko Mikkola for providing me with this interesting subject and sharing their knowledge and expertise. I would also like to thank Chief Engineer Veli-Antti Hakala, Laboratory Manager Jukka Piironen, and the rest of the faculty of the testing hall of structural engineering at the department of civil engineering for their hard work in creating my test specimen, and in helping me conduct the experiments. Special thanks goes also to Kalervo Korpela and all the people from KK-Palokonsultti Oy, for the opportunity to do this thesis, and the chance to work and grow as a fire safety engineer surrounded by wonderful people.

Espoo, November 5, 2018

Henri Kuronen

Symbols and Abbreviations

k	W/(m K)	Thermal conductivity
T	°C or K	Temperature
ρ	kg/m ³	Density
a_1		Constant
a_2	W/(m K ²)	Constant
l	m	Length
α_T	K ⁻¹	Thermal expansion coefficient
m_{water}	kg	Mass of water
m_{wood}	kg	Mass of wood
m_{wet}	kg	Mass of wood and water it contains
m_{dry}	kg	Mass of oven-dry wood
MC	%	Moisture content
RH	%	Relative humidity
u	m ³ /(s m ²)	Volume flux
q	m ³ /s	Flow rate
A	m ²	Area
κ	m ²	Permeability
μ	Pas	Viscosity
p	Pa	Pressure
g	m/s ²	Gravitational constant
J	mole/(m ² s)	Diffusion flux
D	m ² /s	Diffusion coefficient
φ	mol/m ³	Concentration
x	m	position
V	m ³	Volume
n	mole	Amount of substance
R	J/(kg mole K)	Universal gas constant
E	MPa or N/mm ²	Elastic modulus
σ	MPa or N/mm ²	Stress
ϵ		Strain

Contents

Symbols and Abbreviations	5
1 Introduction	8
1.1 Motivation	8
1.2 Problem statement	8
1.3 Structure of the Thesis	9
2 Background	10
2.1 Wood as a construction material	10
2.1.1 Structure and properties of wood	11
2.1.2 Thermal properties	12
2.1.2.1 Heat capacity	12
2.1.2.2 Thermal conductivity	12
2.1.2.3 Thermal expansion	13
2.1.3 The effect of temperature and moisture	14
2.2 The principles behind design methods	16
2.3 Design aspects in practice	17
2.4 Previous studies	18
3 Experiments	23
3.1 Experimental principles	23
3.2 Materials	24
3.3 Heating experiment	29
3.4 Experimental procedure	33
3.5 Results	38
3.5.1 Tensile strength results	42
3.5.2 Elastic modulus results	45
3.5.3 Connection between the tensile strength and elastic modulus	48

4	Simulation model	49
4.1	Motivation and overview	49
4.2	Simulation model and FDS	50
4.3	Python	50
4.3.1	Overview	50
4.3.2	Key locations	51
4.3.3	Post-processing	52
4.4	Example case	53
4.5	Limitations	58
5	Conclusions	60
A	FDS Scripts	64
B	Python Script	95
C	Tensile Test Graphs	101
D	Breakage of specimen	111

Chapter 1

Introduction

1.1 Motivation

When designing timber structures, it is important to understand the phenomena occurring in the load-bearing parts due to the fact that wood is a burning material which chars when it is exposed to high temperatures. When the charring happens, wood loses its structural strength. There are many different methods to assess when wood is completely charred, varying from temperature to certain limits in change of density. However it should be kept in mind that wood starts to lose its strength at temperatures much lower than at which the actual charring happens. This can easily be seen in for example the reduction of its density before reaching the temperature of about 300 °C, which is considered to be the pyrolysis temperature, at which charring is assumed to happen. This weakening of timbers structural strength properties before charring has been taken into account in some extent by Eurocode 5, utilizing an additional reduction of load-bearing dimensions [3]. However this is based on a limited amount of data, but is assumed to be on the safe side. By examining the true load-bearing capability of wood under elevated temperatures, more precise information is to be gained, that will benefit not only the designers, but also the financiers of the building project.

1.2 Problem statement

This thesis focuses on the longitudinal tensile strength properties of timber under elevated temperatures, of which there is only a limited amount of data. Tensile strength is one of the most important mechanical strength properties, alongside with bending and compression strengths. As a structural element, beams are exposed to high tensile strengths as well as to bending. Tensile

strength is also used as a classifier for different strength grades of timber. The objective of this thesis is to complement the underlying patterns of the fire design of timber by taking into account the changes in the mechanical properties of wood before charring, as well as the time dependent charring reactions advancement. This is important, because fire exposures of varying length and magnitude lead to different temperature profiles.

1.3 Structure of the Thesis

The first part, chapter 2, of this thesis consists of a literature study. In this literature study, the main objective is to view and present previous work done on tensile properties of wood under exposure to elevated temperature before charring. First, basic properties of wood are addressed, in order to provide the reader with relevant background information about fire behaviour of wood. A brief look is taken into the design aspects, and how the fire behaviour of wood is taken into account in the Eurocode 5. Then, experimental results from different authors are addressed.

After the literature study, practical experiments are carried out, and will be discussed in chapter 3. In chapter 4, we look into a practical application of the data describing the relationship of temperature and tensile strength. For this purpose, a simulation model and a small software for pre- and post-processing are created. Finally, the conclusions and discussion will be provided in chapter 5.

Chapter 2

Background

2.1 Wood as a construction material

The use of wood as a construction material has become more and more common over the past decades, and will most likely continue this trend in the future. One of the reasons for this is its environmental friendliness. The use of concrete, for example, is much more wearing on environment than using wood and timber products. The effects of choosing building materials become evident because of the fact that the building sector uses 40 percent of total global annual energy consumption and produces 30 percent of total green house gasses [11]. Improvement is needed in our modern, environmentally conscious society. Use of timber could be part of the solution, but in order of that to happen, it is important to understand its properties properly.

2.1.1 Structure and properties of wood

Wood is an anisotropic material, meaning that its properties differ depending on which direction (longitudinal, radial, or tangential) it is reviewed. These different directions are illustrated Figure 2.1.

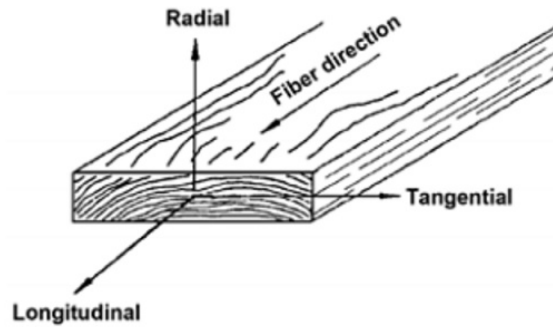


Figure 2.1: The three main directions of wood in relation to the orientation of the grain. [5].

Wood is composed of natural polymers, such as cellulose (a polysaccharide which acts as a skeleton of the material, 50%), hemicellulose (which forms the matrix of the compound, 25%) and lignin (which binds the cells together, 25%). The portions of these three main components (reported as percentage of dry weight) vary depending on the species of the wood [5].

The main focus of this work is on tensile strength, which is one of the most important defining characteristics of the material, and is often used to define the strength class of the wood. Longitudinal direction (parallel to grain) is chosen, as it is the direction wood has the highest tensional strength in, and thus is the most common direction tensional stress is applied to it.

Although wood behaves and is regarded as a viscoelastic material that begins to creep especially during cycles of changing moisture content and temperature [17], these properties take long to become observable. Even for a detection of the phenomenon on a small scale, the time range is usually in days. Thus, the experiments that are performed within this work, are not affected by these properties, as the time range is in minutes.

2.1.2 Thermal properties

Important thermal properties of wood include heat capacity, thermal conductivity, and thermal expansion alongside with its coefficient. In fires, wood is exposed to high temperatures, so understanding these properties is of paramount importance.

2.1.2.1 Heat capacity

Heat capacity c is defined as the amount of energy [J] needed to increase the temperature of a unit of mass [g] by one degree [K or °C]. It is strongly dependent on not only the temperature, but of the moisture content of wood as well. This is due to the fact that water has one of the highest values of heat capacity amongst common substances. However, the effect of species or density of the wood is insignificant [5]. The heat capacity of wood in normal conditions (containing some moisture) consists of the heat capacity of dry wood, water, and additional term accounting for the bonds between wood and water.

2.1.2.2 Thermal conductivity

Thermal conductivity k represents the rate of heat flow through a material subjected to a temperature difference. The thermal conductivity of wood is much lower than that of other common structural materials, not including insulation materials.

Material	Softwood	Steel	Aluminum	Concrete	Glass	Plaster	Mineral wool
Thermal conductivity [W/m*K]	0,10-0,14	45	216	0,9	1	0,7	0,036

Figure 2.2: Thermal conductivities of common structural materials. [5].

Eventhough the species of wood does not directly have an effect on the thermal conductivity, it does so indirectly, as the thermal conductivity is affected by density, moisture content and structural irregularities, which vary among different species. In addition to grain direction, the temperature also affects thermal conductivity, which means that it does not stay constant during real fire conditions, eventhough some pyrolysis models assume so [7].

Multiple researchers have derived different formulas for calculating the thermal conductivity of wood as a function of temperature. These formulas, some of which have been presented below, deviate from one another, as can be seen.

Parker [15]:

$$k = 0,12 \cdot (1 + 0,00091 \cdot T) \frac{W}{mK} \quad (2.1)$$

Kollman [9]:

$$k = k_0 \cdot (1 + (1,1 - 9,8 \cdot 10^{-4} \rho_0)(T - T_0)/100) \quad (2.2)$$

Maku [12]:

$$k = k_0 \frac{T}{T_0} \quad (2.3)$$

Atreya [1]:

$$k = a_1 + a_2(T - T_0) \cdot 10^{-4} \frac{W}{mK} \quad (2.4)$$

where T is the current temperature [$^{\circ}C$], k_0 is the thermal conductivity at room temperature [$W/m \cdot K$], a_1 is a constant depending on the species of wood [$W/m \cdot K$], a_2 is $1,2 W/mK^2$, and $T_0 = 20^{\circ}C$. [14]

2.1.2.3 Thermal expansion

Thermal expansion is defined as

$$\Delta l = \alpha_T * \Delta T * l \quad (2.5)$$

The thermal expansion coefficient α_T describes the relationship between relative change of dimension and change in temperature, which causes it. Here the grain direction has once again a big impact, as the radial and tangential coefficients are 5-10 times larger than that of parallel to grain. They are also proportional to specific gravity, which the latter is not. Thermal expansion coefficient of oven-dry wood parallel to grain does not depend on the species of wood, and its values for both hardwoods and softwoods range from $3,1 \cdot 10^{-6} K^{-1}$ to $4,6 \cdot 10^{-6} K^{-1}$. Unless the wood is initially very dry (moisture content below 4 %), the thermal expansion caused by heating is less than the shrinking caused by loss of moisture. [5]

2.1.3 The effect of temperature and moisture

Moisture content (MC) of wood affects many of its physical and mechanical properties. In literature, moisture content is defined as

$$MC = \frac{m_{water}}{m_{wood}} * 100\% \quad (2.6)$$

or as

$$MC = \frac{m_{wet} - m_{dry}}{m_{dry}} * 100\% \quad (2.7)$$

Moisture content of wood depends strongly on the surrounding conditions, mainly temperature and relative humidity (RH). The figure below shows the correlation between these quantities when the moisture content of wood is in equilibrium, meaning that it is not gaining or losing any moisture. [5]

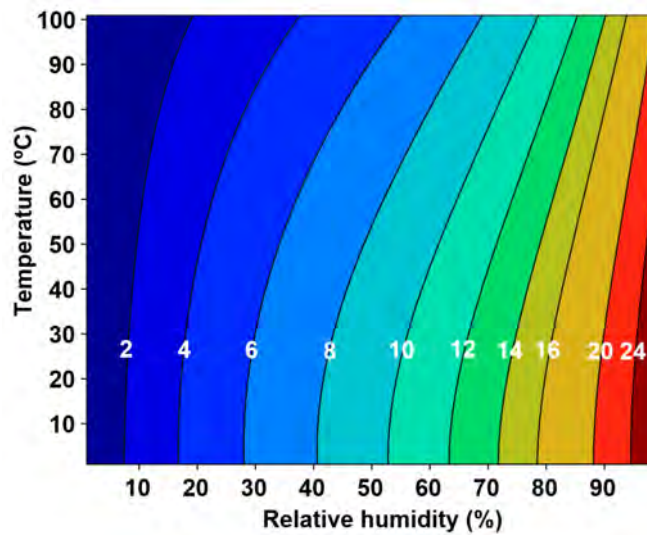


Figure 2.3: Relationship between temperature, relative humidity and moisture content. [5]

When the moisture content of wood decreases below fibre saturation point, it is no longer dimensionally stable and starts to shrink. Below the fibre saturation point moisture starts to exit the cell walls also, and not only from the cell cavities as above this point. The volume of the cell wall depends on how much water is bounded to it, and thus losing this water causes shrinking. As with many other properties of wood, this shrinkage (or swelling if moisture content increases instead of decreasing) is anisotropic. Shrinking

and swelling is greatest in tangential direction, and approximately half of it in radial direction. Compared to these other two directions, longitudinal shrinking/swelling is very small. [5]

When wood is exposed to high temperatures, it starts to undergo the process of thermal degradation. As wood chars, it loses its structural strength. Eventhough the pyrolysis reaction (thermal degradation in oxygenless conditions) which causes the charring of the wood mainly happens around 300°C, the properties of the wood start to weaken long before this.

Up until about 60 °C the mechanical properties of wood don't undergo much change. When the temperature rises up to above 100 °C, the moisture in the wood begins to evaporate quickly. This vaporization of water also causes some of the moisture to move even further into the wood, so it migrates in two opposite directions.

The three main factors causing the movement of moisture in the wood are the pressure gradient, the temperature gradient, and the concentration gradient. The pressure gradient initiates a flow of moisture in the material following Darcys law(1856), which describes this phenomenon for porous material, such as wood.

$$u = \frac{q}{A} = -\frac{K}{\mu} \left(\frac{\partial p}{\partial L} + \rho g \sin \theta \right) \quad (2.8)$$

where u is the volume flux, q is flow rate, A is the area normal to the flow, K is the permeability of the porous media, μ is viscosity, p is pressure, L is the distance in the direction of the flow, ρ is the density of the fluid, g is the gravitational constant, and θ is the angle between flow direction and horizon

Ficks law (1855) gives us a solid foundation for understanding the moisture driven by concentration differences:

$$J = -D(d\varphi/dx) \quad (2.9)$$

where J is the diffusion flux, D is the diffusion coefficient, φ is concentration, and x is the position.

When the volume stays approximately the same, the rise in temperature causes a rise in pressure, which can be stated in the form of the universal gas law. However, in situations involving fire, the vaporization of the water contributes more to the rise of pressure, than just the rise of its temperature.

$$pV = nRT \quad (2.10)$$

If the volume V , amount of substance n , and universal gas constant R stay constant, when the temperature T rises, so does the pressure p . This increased pressure drives the water both into the surface of the wood, and also further into the material. [6]

When the wood has reached temperature of 160 °C, all of its moisture has evaporated, thus making its moisture content (MC) 0 %. [18]

Different components of the wood degrade at different temperature intervals; cellulose between 240-350 °C, hemicellulose between 200-260 °C, and lignin between 280-500 °C. [4]

2.2 The principles behind design methods

In Finland and in other countries which belong to the European union, 'EN 1995 Eurocode 5: Design of timber structures' acts as a basis of fire safety design for timber structures. The recommended method for the determination of cross-sectional properties for the load-bearing capacity of beams and columns is the reduced cross-section method. In this method, an extra reduction of 7 mm is performed on top of the calculated charring depth. This, and the tabulated charring rates give the designer a good basic guideline, which is assumed to be on the safe side. However, using a more precise method could reduce costs by avoiding the excessive use of material. Also, as the dynamics of the fire deviate from the standard fire situation, designs made in-line with the Eurocode may pose a risk to safety.

The other method given by Eurocode is the Reduced properties method. In this method, the reduction of 7 mm layer is not done. Instead, the strength and stiffness properties of the timber are modified. This is done via modification factor $k_{mod,fi}$. The values of the properties are multiplied with this modification factor, and thus new, reduced, properties are gained and used in the design.

In addition to these, annex B of EN 1995-1-2 goes through an advanced calculation method, which can be applied to get the temperature within the structure (thermal response model), and a more accurate estimate of the charring depth and rate. The relationship between rise of temperature and strength properties introduced in this annex is illustrated in the figure 2.4. [3]

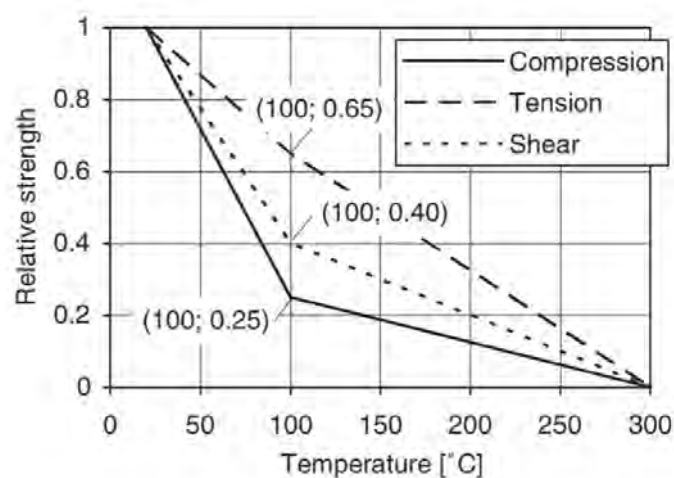


Figure 2.4: The relation of temperature and strength properties parallel to grain in softwoods. [3]

2.3 Design aspects in practice

When designing a structural element, whether it is a beam, a column, or a frame, its cross-sectional area and dimensioning is often dictated by the loads it is subjected to. Different load combinations and stresses they produce (tension, compression, bending, torsion and shear) are evaluated, and based on these, a critical stress is identified. Then the structural element is dimensioned accordingly. In case of timber structures for example, the cross-sectional area can be increased in order to enhance the structure's fire performance.

An unpredicted reduction in the strength properties of a structure can be dangerous, as the structure may be subjected to more stresses than it can handle. If the reduction of strength does not happen homogeneously, it can cause the critical stress to be different, and elsewhere than predicted during the design process. This kind of behaviour can occur for instance during a fire. Without the proper tools and data available, it will be very hard for a structural engineer to anticipate such an event, not to mention preventing it from happening.

A solution for such a problem may be found in a more effective combining of knowledge between structural designers and fire safety engineers. By utilizing FEM-modelling (Finite Element Method), the structural engineers can accurately model the structure and the stresses it is under. A deeper analysis

will reveal the internal stresses within the component, at a point (or points) of interest. The fire safety engineer could then contribute by analyzing how the design fire will increase the temperature of the structure, and create a temperature profile of it. Based on the temperature profile, we can link relative strength to each point throughout the structure. Then, by combining both of these, an analysis can be made on which parts of the structure fail to meet their design criteria, and under which type of stress.

Mainly this approach would be practical and useful in building projects of Finnish fire class P0, which need their fire safety demonstrated using analysis based on the assumed fire development. These buildings do not follow all the structural guidelines stated and tabulated in the Eurocode or the Decree by Ministry of the Environment on fire safety of buildings, 848/2017, which came in to effect 1.1.2018 as the new fire safety regulation [21]. Because of this, the fire design will be based on design fire scenarios, which are often simulated, and thus getting relevant data for the structural analysis would not take an unreasonable amount of extra work.

2.4 Previous studies

Most of the studies conducted on the fire behaviour of timber focus on charring. Still, there are a few studies concerning behaviour of wood at elevated temperatures, which do not involve charring. One of the most famous of these is the research conducted by König [10]. His study on the effect of temperature on elastic modulus and strength properties of wood have been recognized by CEN (Comité Européen de Normalisation, or European Committee for Standardization in English) and taken into account in the Eurocode 5.

In 1985 B.A. Östman conducted a study [2] on the tensile strength of wood at temperatures and moisture contents simulating fire conditions. She carried out her experiments with spruce (*Picea excelsa*) in temperatures up to 250 °C, with a moisture content varying between 0 and 30 % (moisture content in temperatures above 100 °C was 0 %, because of the vaporization of water). Based on the results, she deduced that both temperature and moisture content have a significant effect on the tensile strength of wood, and thus should both be taken into account. With a moisture content of 30 %, when the temperature of the spruce samples rose from 25 °C to 90 °C, the tensile strength of wood may only be about 50 % of its original value. When dry samples were examined, it was observed that at 200 °C the tensile strength had decreased to 60 % and at 250 °C to 40 % of its original value at 25 °C. [2] Figures 2.5 and 2.6 demonstrate the differences in the experimental

data gathered by different researchers.

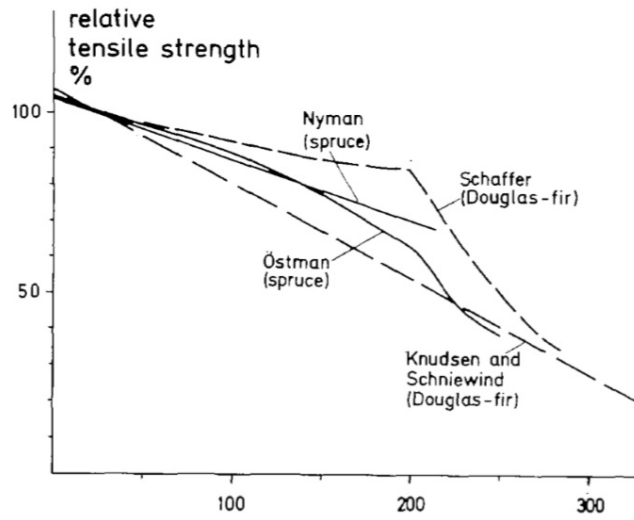


Figure 2.5: Graphical representation of results by Östman, in comparison with other studies. [2]

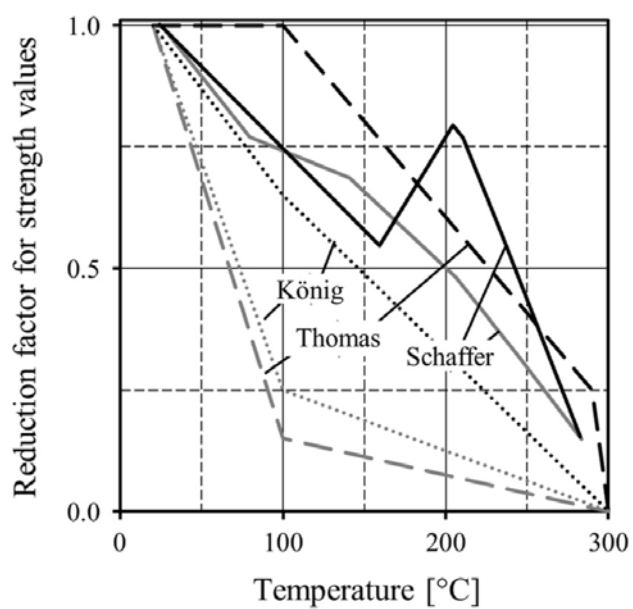


Figure 2.6: Graphical representation of the variation of compressional (grey lines) and tensional (black lines) strength as a function of temperature. [19]

Östmans results thus show greater tensile strength than those of König, which are included in the Eurocodes. The results by König should be valid for softwoods, which spruce belongs to (although, species of wood are not itemized in the Eurocode). Thus, the Eurocode seems to be overly-conservative. This is good for safety, but bad from an economical point of view.

Due to the low thermal conductivity of wood and especially char, the temperature gradient inside wood is very steep, and thus its thermal penetration depth is relatively small. After circa 20 minutes of standard fire exposure, the heat-affected thermal penetration zone is approximately 40 mm deep, and within it the temperature changes from circa 300 °C to 20 °C (assuming that 20 °C is the temperature of the environment). This is illustrated in the figure below.

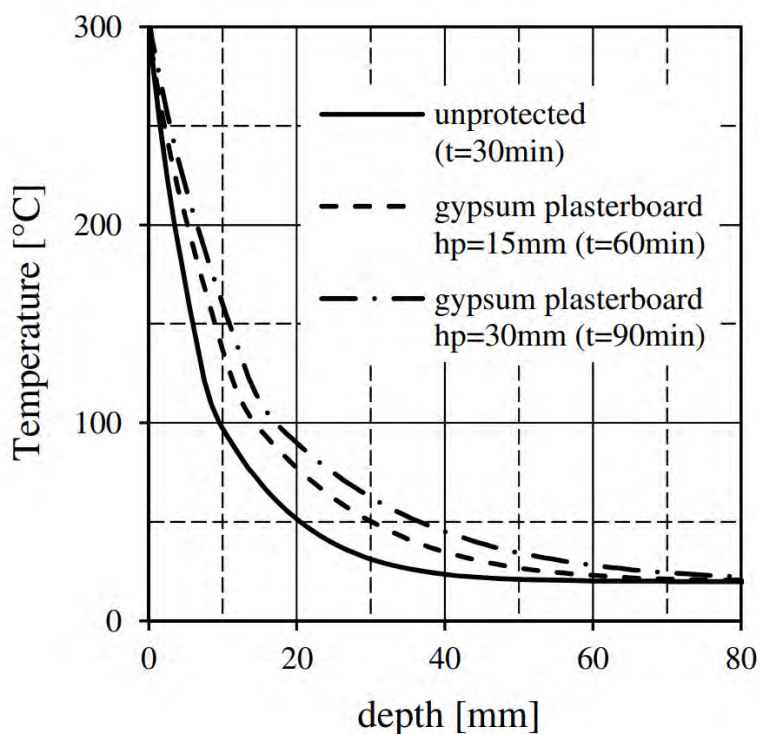


Figure 2.7: Temperature profile within wood. [19]

Unlike with e.g. steel, each point in this heat-affected area has differentiating strength and stiffness properties, because of the material properties of wood. Based on this lower-strength layer, the RCSM (Reduced Cross-Section Method, published in the 1980s) simplifies a layer with zero-strength, zero-strength layer, which has no structural strength or stiffness, deeming the rest of the heat-affected zone structurally unchanged [19]. This approach assumes that the zero-strength layer thickness remains the same 7 mm after 20 minutes of fire exposure (up to which it rises steadily) [3]. After this time, the thermally insulating char layer thickens as the surrounding temperature grows, keeping the temperature profile of the heat-affected zone approximately constant.

However, there is almost no data confirming this with fire exposure times of 60 minutes or longer and none after 90 minutes. [19] This wide applicability and openness for interpretation raises the possibility for both over- and under dimensioning, which can lead to reductions in safety or monetary gains.

Data by different researchers differ from each other quite a bit, and taking into consideration that Eurocode 1995-1-2 has temperature dependent reduction factors in strength properties produced by König, clearly consideration and further inspection and experiments into these properties is needed. This will be tackled in the next chapter.

Chapter 3

Experiments

3.1 Experimental principles

For the purpose of this thesis and confirming the relationship between tensile strength and temperature, tensile tests were carried out at different temperatures. The experiments were conducted with 56 spruce samples at a constant temperature as a steady-state test, increasing the tensile stress until breakage. In order to get data on the effect of temperature, the experiment was conducted at different temperatures, with an interval of 25 °C. Eventhough 300 °C is considered to be the pyrolysis temperature at which the wood chars, decomposition of wood can happen well before reaching this temperature. This is why the experiments were only conducted up to 250 °C. In order to increase the reliability of the results, three individual tests were carried out at each temperature, for both oven-dry and moist samples. When the sample has reached the temperature of 125 °C, all moisture can be assumed to have evaporated, and these samples are considered to be oven-dry. Still, also moist samples were tested at each temperature, in order to prove this assumption, and also to increase the number of samples, thus reducing the significance of randomness. The moist samples had been stored in a room with RH 45 and temperature of 20 °C. This was done to represent real life conditions, at which the timber structures often are. The moisture content of the samples was defined by oven drying and weighing the samples before and after. The test matrix below visualizes the conditions of the tensile tests conducted.

Temperature (°C)	Oven dry samples (pcs)	RH 45 samples (pcs)
Room temperature	4	4
75	3	3
100	3	3
125	3	3
150	3	3
175	3	3
200	3	3
225	3	3
250	3	3

3.2 Materials

The samples were produced from spruce. Spruce was chosen, because it is a common species used in structural products, such as CLT and glulam. At the narrowest part, where the tensile failure is presumed to occur, their dimensions were approximately 20 mm x 7 mm. The sample-specific variation was measured for each sample, and taken into account. The sample is shown in figures below.

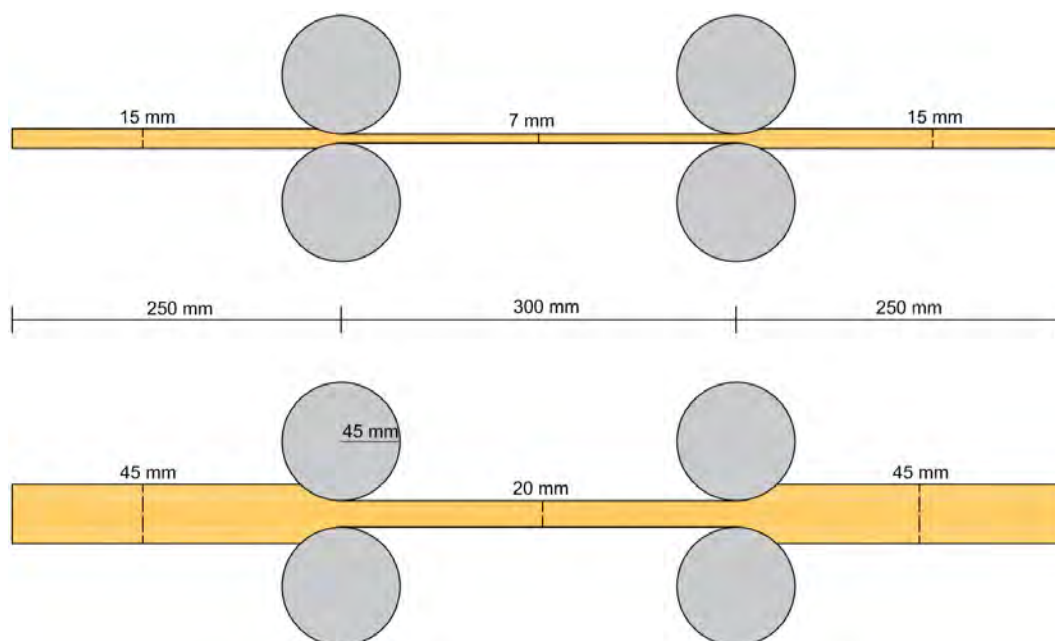


Figure 3.1: Dimensions of the spruce sample



Figure 3.2: Spruce samples

The weight of the samples was measured both after the storage in RH45 room, and after the oven-drying. The weight data of the oven-dried samples is presented in the table below. The variation in the weights between the samples is caused by both variation in the density, which is due to varying grain thickness and the presence of knots, and the small variation in dimensions of the samples. The moisture content was then defined as the ratio between the weight of the water and the weight of the sample after drying. As can be seen, the moisture content of all the samples is approximately 10 % (the average was 10,3 %, with a standard deviation of 0,2 %), which corresponds relatively well to the relationship between temperature, relative humidity and moisture content presented earlier in the figure 2.3. Eventhough the moist samples were not dried and weighed, we can assume that they also have similar moisture content. In order to maintain the moisture content of the samples outside the RH45 room, the samples were sealed into a plastic pouch shown in the figure below.



Figure 3.3: Samples sealed within the plastic pouch

Specimen ID	Weight before drying [g]	Weight after drying [g]	MC [%]
Ovendry 1	182,9	166,0	10,18
Ovendry 2	163,0	147,5	10,51
Ovendry 3	157,9	142,8	10,57
Ovendry 4	171,5	155,6	10,22
75 D	170,0	154,6	9,96
75 E	157,2	142,7	10,16
75 F	144,9	131,7	10,02
100 D	166,9	151,7	10,02
100 E	149,2	135,4	10,19
100 F	147,4	133,8	10,16
125 D	173,5	157,8	9,95
125 E	173,9	157,5	10,41
125 F	159,4	144,5	10,31
150 D	160,2	145,6	10,03
150 E	165,1	149,4	10,51
150 F	163,5	148,2	10,32
175 D	145,2	131,8	10,17
175 E	165,3	150,5	9,83
175 F	154,3	139,6	10,53
200 D	148,6	134,4	10,57
200 E	156,9	142,1	10,42
200 F	158,7	143,8	10,36
225 D	157,4	142,7	10,30
225 E	150,6	136,6	10,25
225 F	178,7	162,0	10,31
250 D	156,1	141,4	10,40
250 E	163,0	147,6	10,43
250 F	159,2	144,7	10,02

In order to ensure the homogenic temperature profile throughout the sample, the sample had to stay in the oven for a fixed time before starting the actual experiment. This fixed time was determined via simulations. Taking into account the temperature-dependent conductivity and heat capacity of spruce, an FDS (Fire Dynamics Simulator) model was built. Because FDS models 1D heat transfer most accurately, the model was simplified to this from the actual experimental setup. In the actual experiments, the heat is transferred into and in the wooden sample in all directions. As a first simplification of the model, it can be assumed that only the heat transferred from both sides of the narrowest, 7 mm, part is relevant. This 2D approach can be further simplified to 1D, by taking into account only the heat transferred from the other side, and reducing the thickness the heat has to travel inside the wood to 3,5 mm. This was simulated by modeling a closed space (furnace), the temperature of which was set to represent each of the different experiments (75 °C, 100 °C, 125 °C..). On the bottom of this space was a wooden plate. Temperature inside this plate was measured in the simulation in order to see when the temperature at the depth of 3,5 mm had reached its target value. Since the approximations made in transferring from 3D to 1D were all on the conservative side, it can be said that the simulations represent the worst case scenario, and the real sample will most likely be at the target temperature before the sample in the simulation.

It was decided that adequate target temperature was reached, when;

$$T_{Sample} = T_{Furnace} \pm 1^{\circ}C \quad (3.1)$$

The starting temperature T_0 was assumed to be 20 °C. In the test hall, it was later measured to be 25 °C, meaning that especially with the smaller target temperatures, the samples would reach the adequate test temperature sooner. The times it took for each simulation to reach this temperature, are tabulated and graphed below. The explanation for the shorter times towards higher temperatures can be found in the fact that the conductivity of wood increases as temperature rises.

Furnace temperature [°C]	Target temperature of the sample [°C]	Time [s]
75	74	851
100	99	852
125	124	837
150	149	811
175	174	782
200	199	751
225	224	720
250	249	698

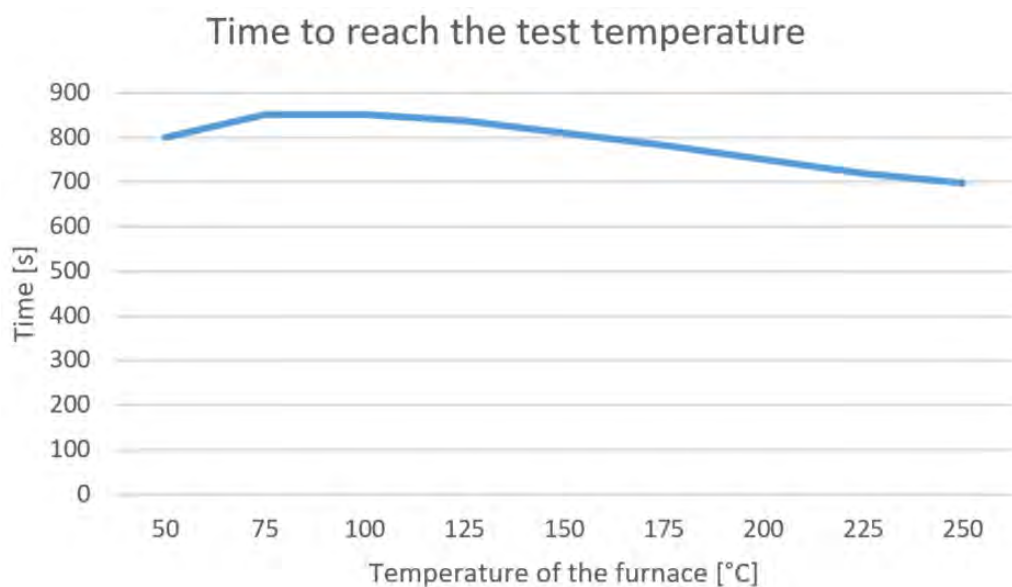


Figure 3.4: Simulated time for the sample to reach test temperature

These simulations work as a good basis for evaluating the heating process. However, when the furnace was introduced to the setup, it became clear that the temperature rise within it needed to be relatively slow. This was due to the fact that otherwise the furnace might overheat and the wooden sample within might behave unpredictably. This issue is addressed in the next subchapter.

3.3 Heating experiment

In order to concur that the temperature rise within the samples matches the results of the simulation, an experiment was conducted. In the experiment, four thermocouples were attached to the sample. This is shown in figure 3.5.



Figure 3.5: Thermocouples placed within the sample

Thermocouples 1, 2 and 3 were placed within the center sample, as shown in the figure. This was done by drilling a small hole, and fitting the thermocouple tightly into it. The fourth thermocouple was placed on its surface. The temperature within the furnace was raised at a rate of $5\text{ }^{\circ}\text{C} / \text{minute}$. This heating rate was also later used in the actual tensile strength experiments. This preliminary test was conducted at temperatures of 50, 100, 150, 200 and $250\text{ }^{\circ}\text{C}$. The results of the thermocouple measurements of each test are shown in the figures below.

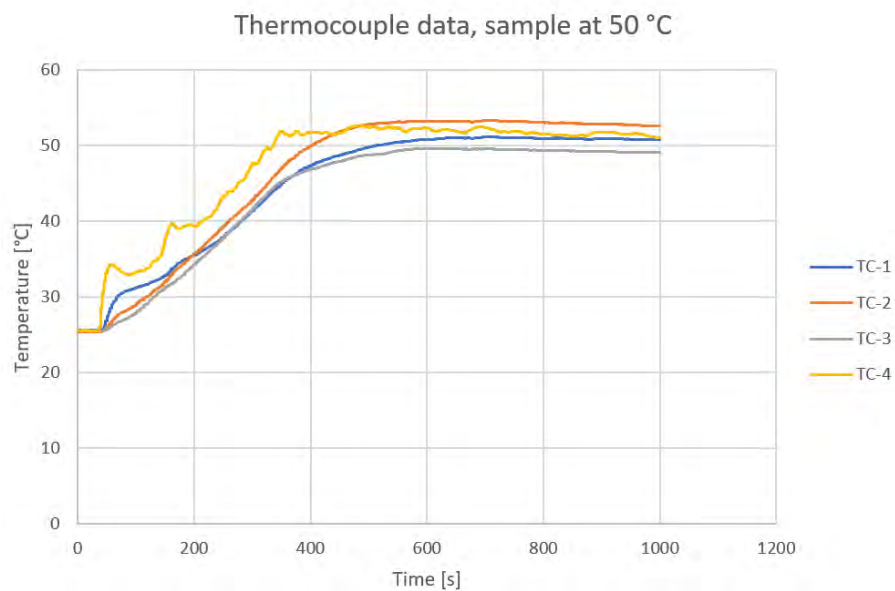


Figure 3.6: Thermocouple measurements with the furnace set to 50 °C.

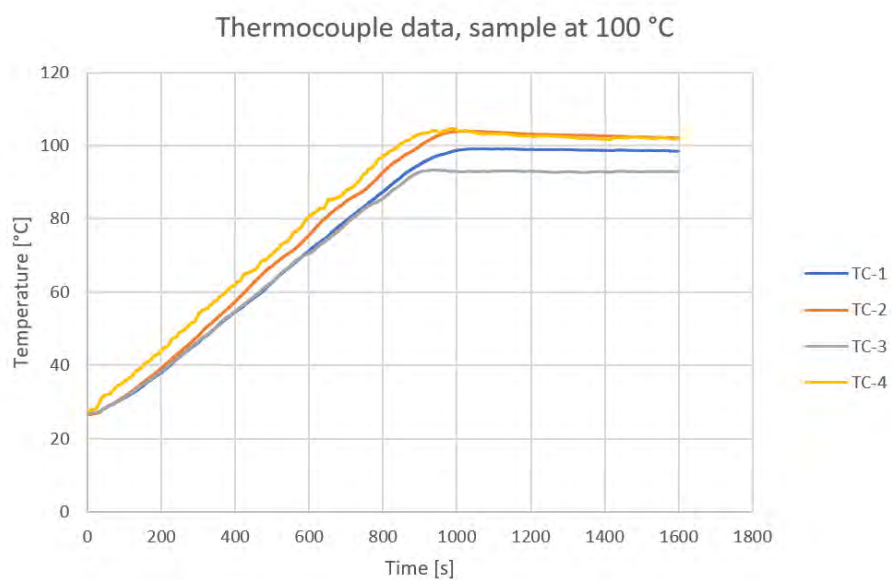


Figure 3.7: Thermocouple measurements with the furnace set to 100 °C.

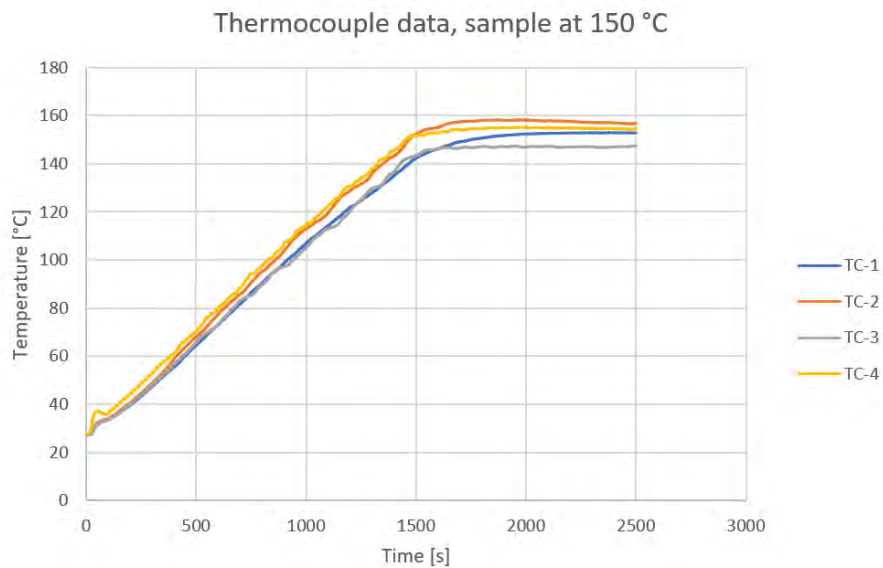


Figure 3.8: Thermocouple measurements with the furnace set to 150 °C.

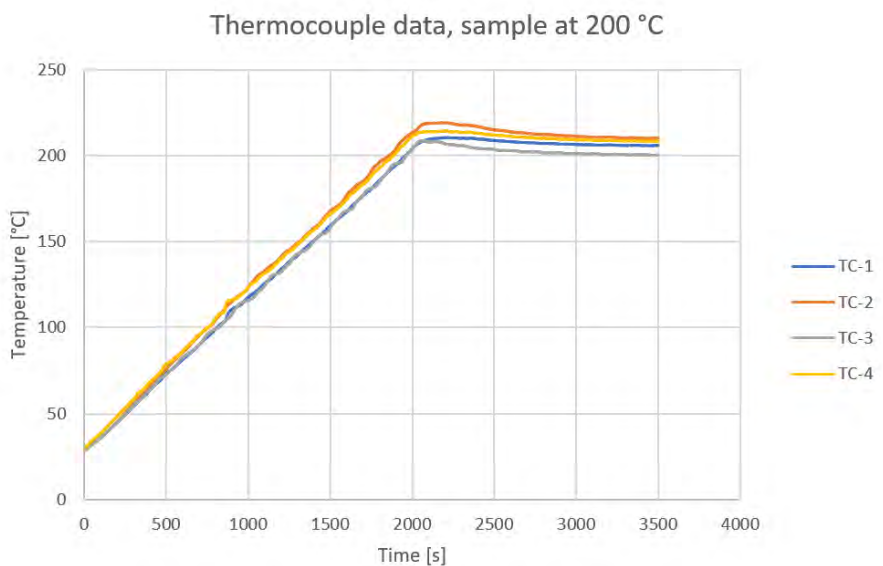


Figure 3.9: Thermocouple measurements with the furnace set to 200 °C.

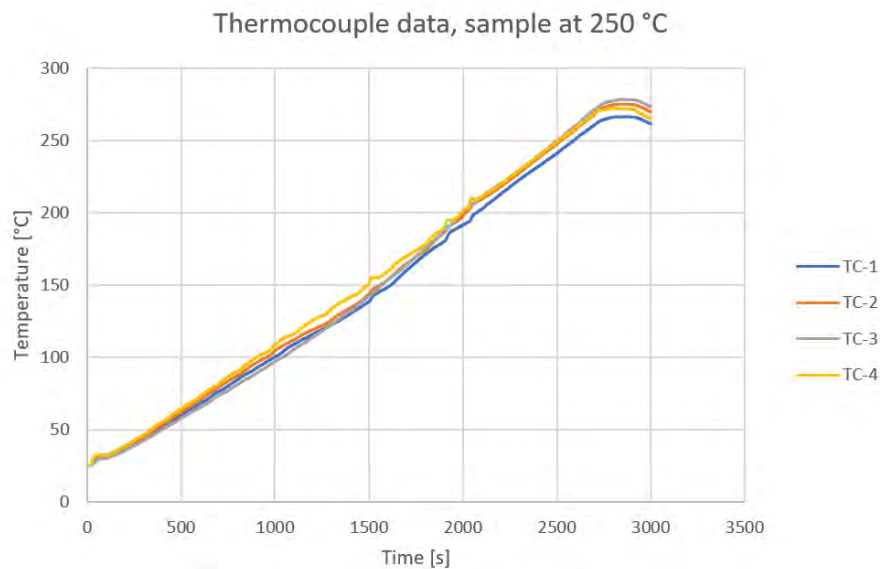


Figure 3.10: Thermocouple measurements with the furnace set to 250 °C.

Based on the results of the heating tests, it was deemed that an adequate temperature profile within the sample is reached in five minutes of the furnace reaching its desired temperature. When compared to the simulations, we see that the simulated times were on the safe side. The inaccuracy and heterogeneity of the temperature profile within the sample can also be seen in the results. A variation of approximately 10 °C is visible in the results, and it increases as the furnace is heated to higher temperatures. In figure 3.10 are the results of the test with the furnace set at 250 °C, in which the actual temperature within the sample peaked at approximately 275 °C. This kind of variation may be caused by the differences within the temperature profile of the furnace itself, by internal variation in properties of the material in the sample, or by the installment of the thermocouples. This sort of uncertainty of the temperature is to be taken into account whilst interpreting the results of the tensile strength experiments.

3.4 Experimental procedure

Before the beginning of the actual tensile test experiment, the sample was put under a pre-load of 100 N. This is done to firmly lock the sample into place, before the actual measurement of the strain starts. The tests were performed as position controlled, with a speed of 0,00005 1/s, at which the upper clamp was set to move. The loading speed was chosen in order to cause the breakage of the sample at approximately 5 to 10 minutes into the tensile test. The tension was created into the sample by attaching it to two clamps, with the uppermost moving and the one on the bottom fixed into place. The attachment of the sample is shown in the figure below.

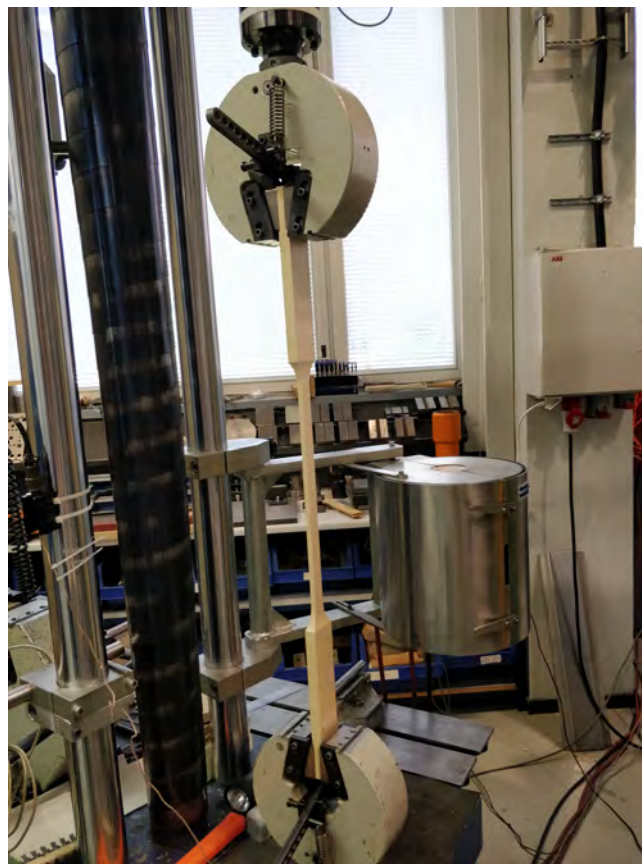


Figure 3.11: The attachment of the sample into the clamps

When conducting the tensile tests in room temperature, the strain was measured with an MTS Axial Extensometer. The strain could have been also measured from the separation between the clamps, but this would have been more inaccurate.



Figure 3.12: MTS Axial Extensometer 634.11F-24

After the experiments in room temperature, the furnace was introduced into the setup. The extensometer could not be placed within the furnace, as it does not respond well to high temperatures. This problem was resolved by switching the extensometer to a model which has the unit outside the furnace, with ceramic measuring rods extending into the oven. This is illustrated in the figures below. Based on the results of the heating experiments, the sample was placed within the furnace, which was then heated up $5\text{ }^{\circ}\text{C}$ /minute to target temperature. After five minutes of reaching this temperature, the tensile test was started.



Figure 3.13: Sample within the furnace

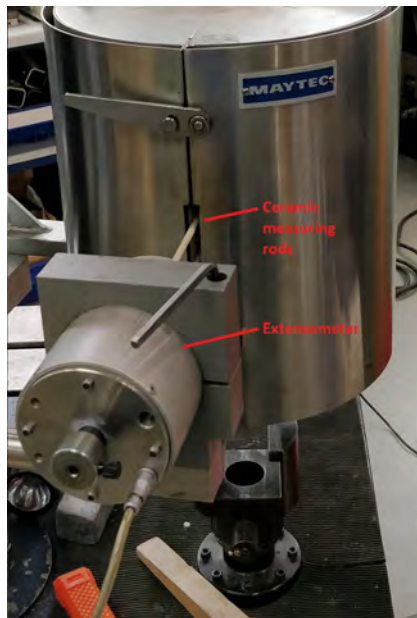


Figure 3.14: Attachment of the extensometer

In order to fix the measuring rods into the sample, a pair of demec-thumbtacks were glued to the centerline of the sample with heat-resistant glue, 5,08 cm (two inches) apart from each other. This is illustrated in the figure below.



Figure 3.15: Demec-thumbtacks at the center of the sample

Figure 3.16 illustrates the ending of an experiment at 225 °C. The tensile strength experiments were all ended when the force applied to the sample dropped below 50 % of its maximum value. This is why some of the samples, like in the figure, seem to be in one piece. In the picture we see both the measuring rods and the spots they were attached to, before they were retracted for their safety. We also see the insulation at the top and bottom of the furnace, used to keep the temperature within as steady as possible. The wooden sample itself has changed color due to the exposure to high temperatures.

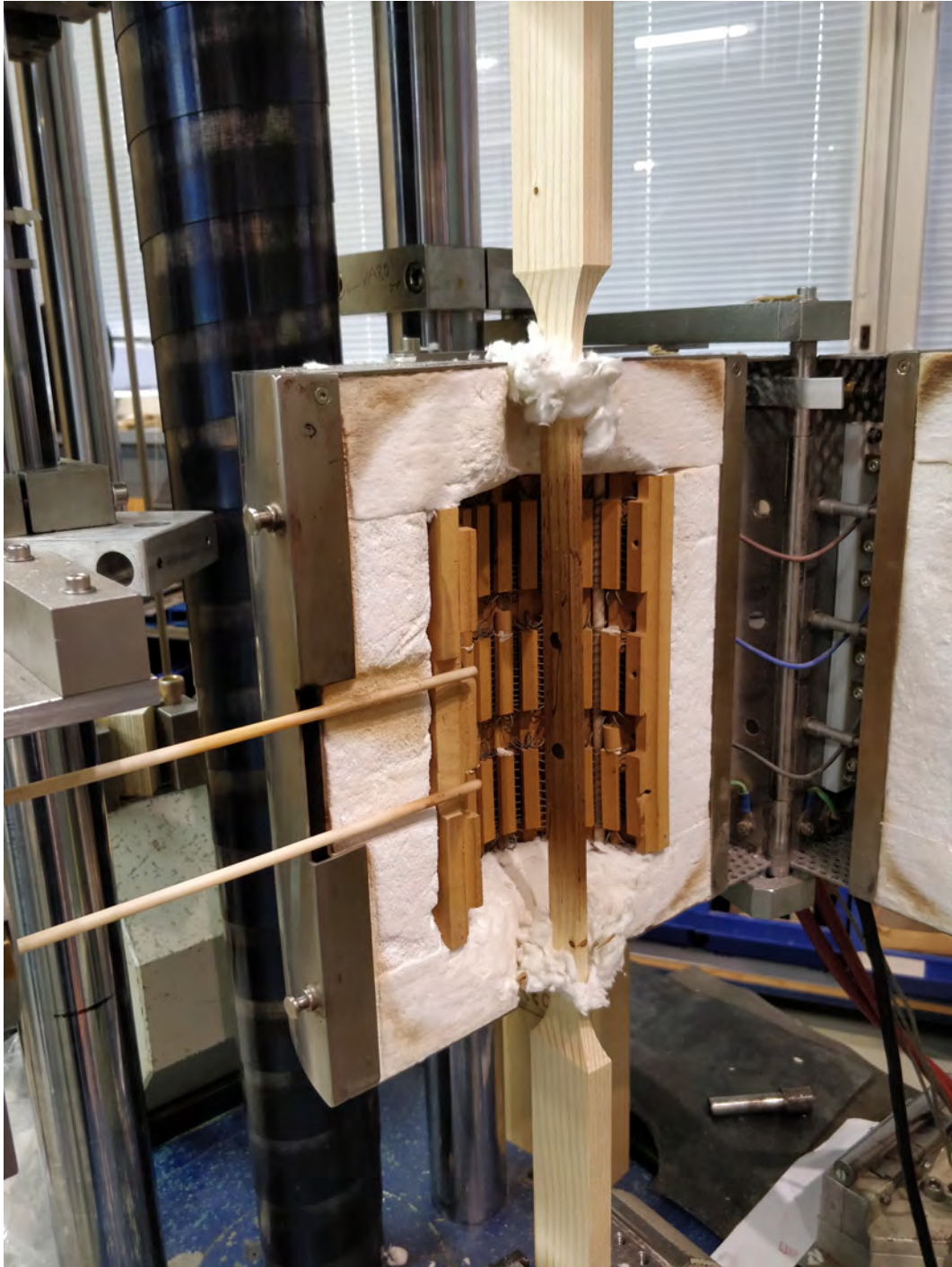


Figure 3.16: End of experiment 225 E

3.5 Results

To ensure that the fragile ceramic measuring rods would not break, the measurement of the strain was terminated well before the breakage of the sample. From the data gathered, the elastic modulus was defined as

$$E = \frac{\sigma}{\epsilon} \quad (3.2)$$

where σ is the uniaxial stress in Pa, and ϵ is the unitless strain (change in length divided by original length). Below we see the tensile strength and elastic modulus data tabulated. The temperature of each test is presented as the first digits of the specimen ID, and letters A-C correspond to moist samples, D-F oven-dry. Tests with specimen ID "Room temperature" and "Oven-dry" were conducted at the testing hall room temperature, which was measured to be approximately 25 °C.

Specimen ID	Tensile strength [MPa]	Elastic modulus [MPa]
Room temperature 1	86,77	13070
Room temperature 2	75,75	12560
Room temperature 3	53,11	13110
Room temperature 4	126,68	16400
Oven-dry 1	69,11	12470
Oven-dry 2	79,87	15100
Oven-dry 3	78,61	14090
Oven-dry 4	88,10	15600
75 A	84,01	17390
75 B	83,82	Not defined
75 C	36,70	13350
75 D	67,39	24080
75 E	97,64	Not defined
75 F	46,02	16400
100 A	68,49	14950
100 B	40,93	13190
100 C	80,08	Not defined
100 D	68,41	Not defined
100 E	47,95	8010
100 F	74,97	Not defined
125 A	49,38	20990
125 B	93,71	29400

125 C	77,59	Not defined
125 D	70,40	14440
125 E	33,81	Not defined
125 F	49,05	11690
150 A	25,23	10670
150 B	53,15	Not defined
150 C	25,50	7590
150 D	91,26	19570
150 E	57,32	6170
150 F	62,69	11160
175 A	28,67	7860
175 B	37,21	5940
175 C	51,51	10010
175 D	37,54	5270
175 E	45,27	Not defined
175 F	36,98	6220
200 A	39,80	9510
200 B	29,48	3950
200 C	7,54	3310
200 D	13,94	5580
200 E	41,55	Not defined
200 F	26,54	7600
225 A	23,44	4960
225 B	27,18	Not defined
225 C	9,57	1560
225 D	15,95	4190
225 E	38,74	4660
225 F	30,12	6930
250 A	26,94	4300
250 B	5,95	1490
250 C	9,57	2160
250 D	18,25	970
250 E	25,90	6600
250 F	14,36	2910

As can be seen, there are multiple occasions in which the modulus of elasticity could not be calculated. This is due to a clear error in the measuring process, for example slipping of the ceramic rods from the demec thumbtacks, or some other unexplainable event. The figure below illustrates the strain measurements of specimen 75 A and 75 B, in which the undefinability of the modulus of elasticity is clarified.

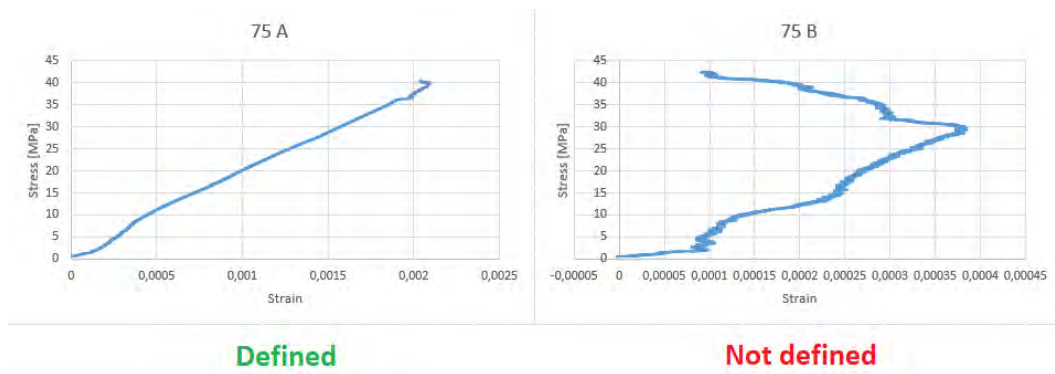


Figure 3.17: Data with definable and undefinable modulus of elasticity

With data from which the definition of modulus of elasticity is possible, such as 75 A, the modulus of elasticity is defined by choosing two points between which the strain is linear. Then a line is fitted through these points, and the slope of this line is the modulus of elasticity. This principle is illustrated in figure 3.18. When interpreting the results, the uncertainty caused by this method should be taken into account.

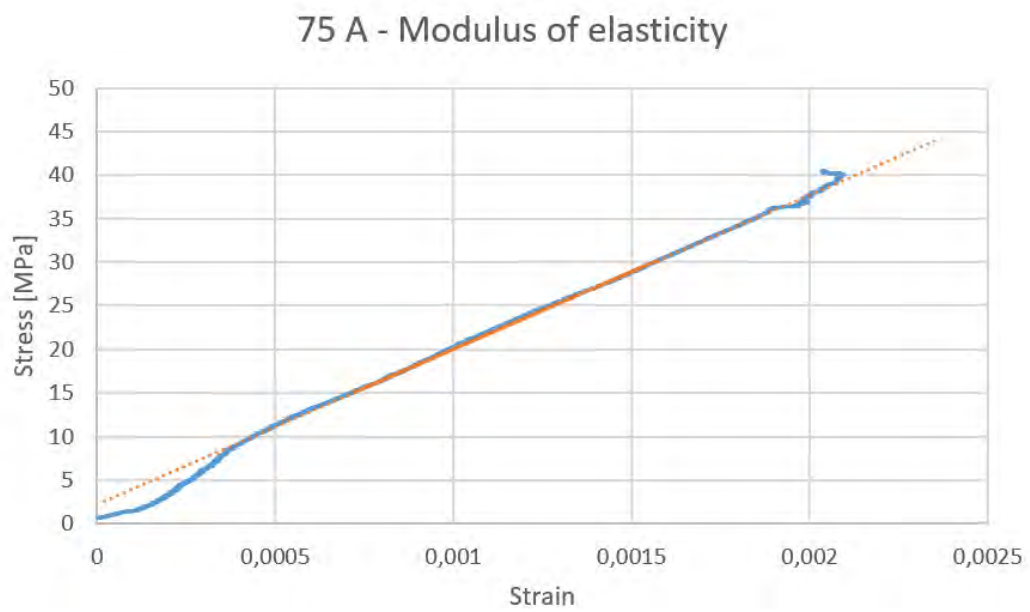


Figure 3.18: The principle of defining the modulus of elasticity from the experimental data

3.5.1 Tensile strength results

The results regarding the tensile strength are visualized in the figure below. Ovdried samples are shown with an orange dot, and the moist samples with a blue dot. When comparing the placement of these data points, the effect of moisture content can not be specified. This is due to the fact that the variation of tensile strength between each samples is too big. With a larger number of specimen, the effect of the moisture content would most likely be observable.

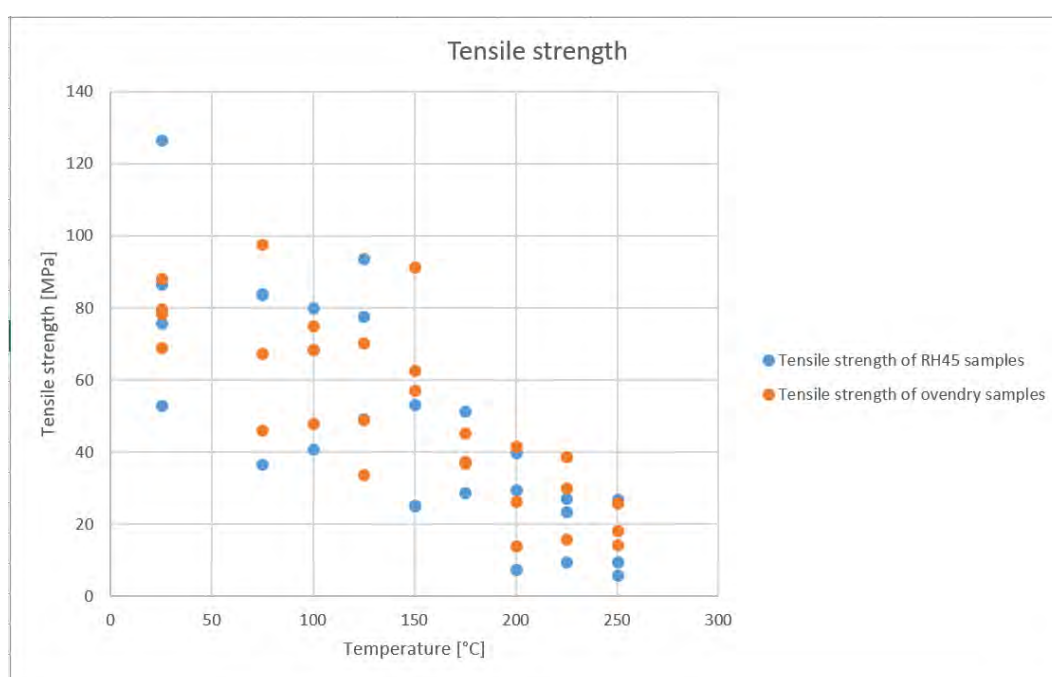


Figure 3.19: Illustration of all datapoints of the tensile strength experiment

As can be seen, there is a clear reduction in the tensile strength as temperature rises. When we take the average for the results for each test temperature, we can fit a line with the value of the coefficient of correlation, R^2 , 0,9703. This means, that the fitted line matches the dataset well (for a perfect match, the coefficient of correlation would be 1). This is shown in the figure 3.20.

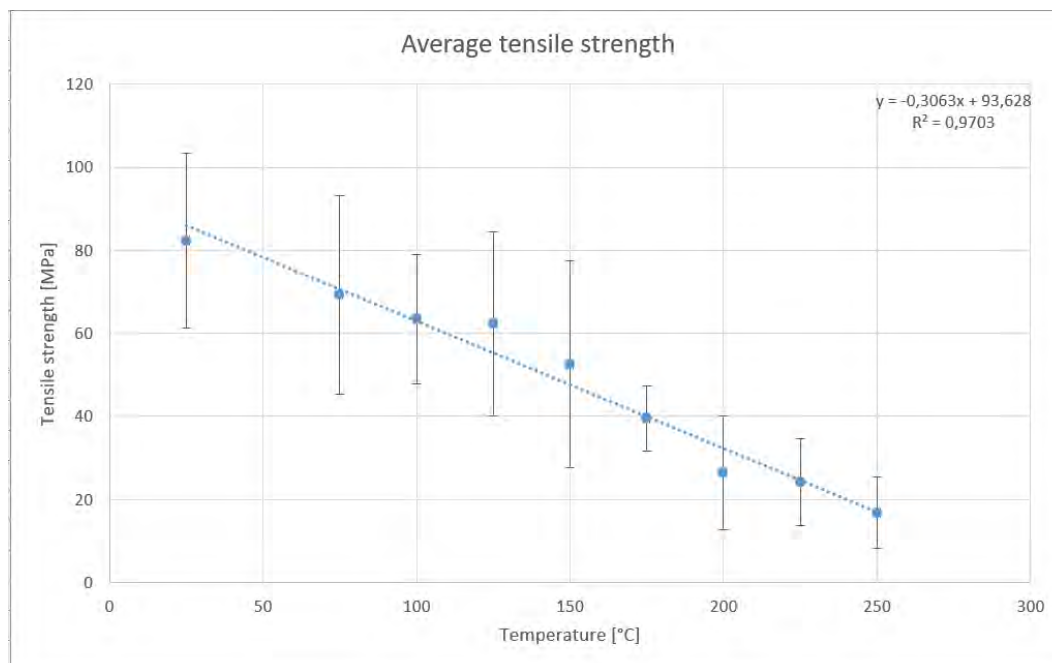


Figure 3.20: Averaged tensile strength of each test temperature

The standard deviation for each averaged value is also shown in the figure. Standard deviation is calculated as

$$SD = \sqrt{\frac{\sum(x - \bar{x})^2}{(n - 1)}} \quad (3.3)$$

where x goes through all the measured values of tensile strength, \bar{x} is the average tensile strength, and n is the number of samples. As can be seen, the standard deviation is quite large. By increasing the number of samples it might get smaller, provided that the data begins to gather more tightly around the average, resembling e.g. the Gaussian distribution.

Now, we can compare this fitted line with the reduction of tensile strength presented in Eurocode EN 1995-1-2. The reduction is given as percentage of maximum tensile strength, so a little fitting needs to be done. This is achieved by using the equation of the fitted line from experiments to find the value of "maximum strength" at 20 °C. This comparison is illustrated in the figure below.

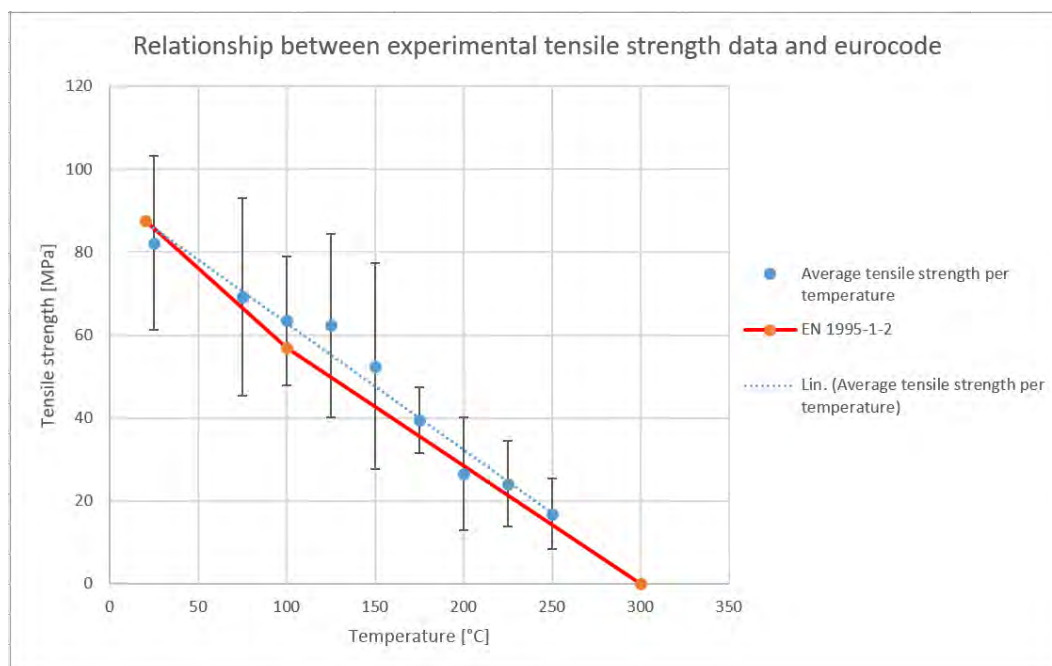


Figure 3.21: Comparison between the eurocode and the experimental data

Eventhough there was a large variation in the data, the averaged values of tensile strength fit the values presented in the eurocode surprisingly well. However, trends such as the change in slope of the eurocode can not be found in the experimental data. By conducting a larger amount of tests, such trends might arise. Also, as the amount of samples increases, standard deviation may decrease. This is why the subject should be investigated further, with a considerably larger amount of specimen. Because the standard deviation of the averaged experimental results is on both sides of the plotted Eurocode data, it can't be stated that the Eurocode is on the safe side, which could be the first conclusion by only viewing the averaged data without its standard deviation.

3.5.2 Elastic modulus results

Out of all 56 tensile tests, in 45 it was possible to define the modulus of elasticity. The figure below illustrates the data gathered, with the oven-dry samples noted as orange dots, and the moist samples with blue ones. Similarly to the tensile strength data, the number of specimen is too low for the effect of moisture content to show up in the data.

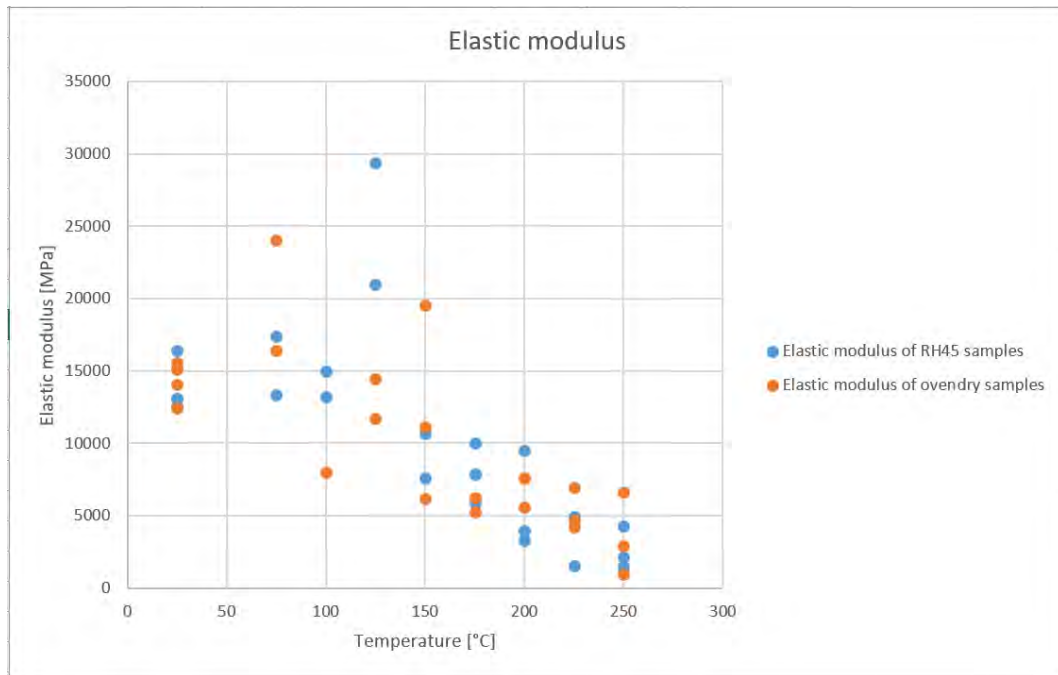


Figure 3.22: The modulus of elasticity data

As the temperature increases the modulus of elasticity decreases, similarly to the tensile strength. This is further visualised in figure 3.23, with averaged elastic modulus for each temperature set. As can be seen, the data has more variation than the tensile strength data, thus leading to a smaller value for the coefficient of correlation R^2 . However, the decreasing trend is clearly visible. Standard deviation is calculated for each data point using the same principle as with tensile strength data. The deviation is large, but as can be seen, it decreases towards higher temperatures.

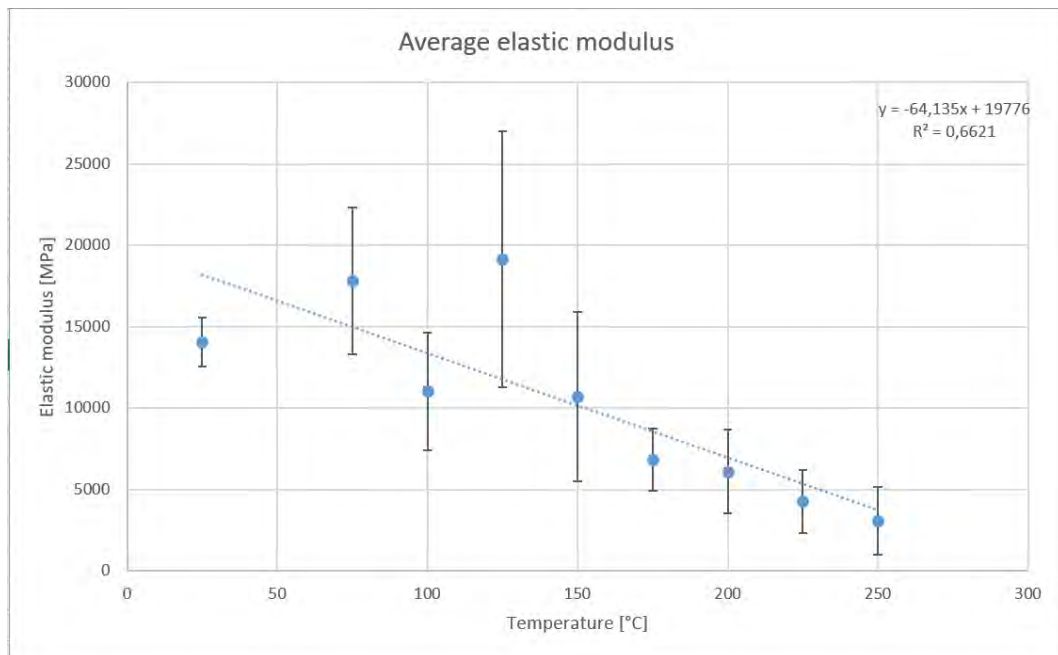


Figure 3.23: The modulus of elasticity data averaged for each temperature

Eventhough the line fitted to match the points is only a rough approximate with a constant slope, it compares to the eurocode relatively well, as can be seen in figure 3.24.

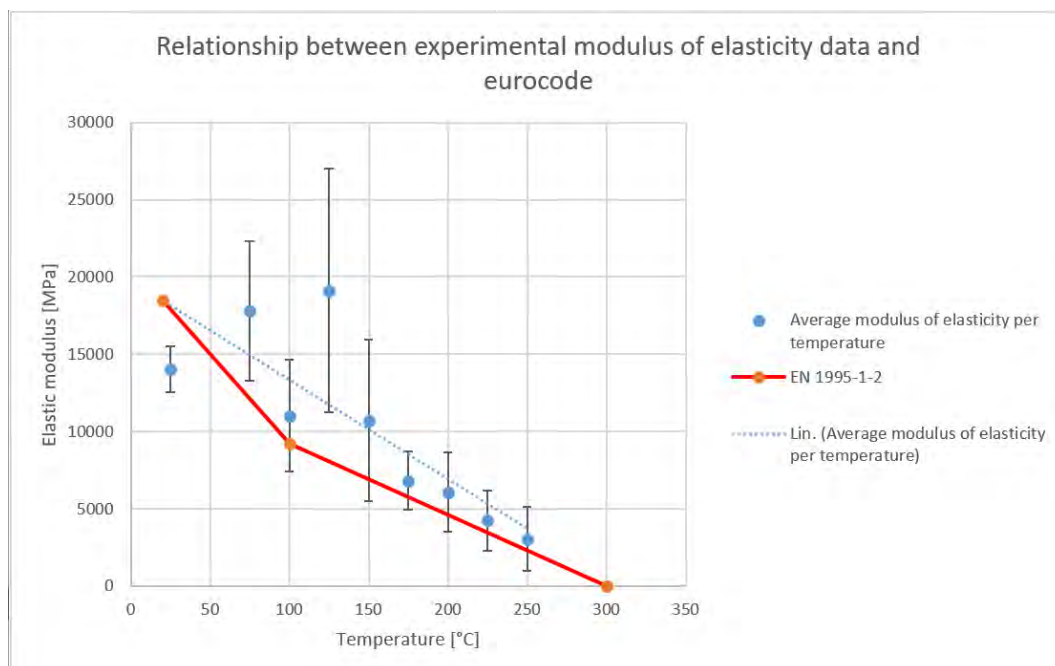


Figure 3.24: The modulus of elasticity data averaged for each temperature compared to the eurocode

3.5.3 Connection between the tensile strength and elastic modulus

As we have established in the previous subchapters, both the modulus of elasticity and the tensile strength decrease as a function of temperature. Thus, there is a clear correlation between these two, which raises the question, is there a causality, i.e., does one cause the other. This can be investigated by looking at the test data gathered within the same temperature. The figure below illustrates the relationship between the modulus of elasticity and tensile strength. As can be seen, overall when the modulus of elasticity increases, the tensile strength of the specimen tends to also increase. When we look at the lines plotted for each temperature, we see only positive slopes. This means that within a constant temperature, as the modulus of elasticity increases, so does the tensile strength. This proves a causality between these two quantities, now with temperature taken out of the equation.

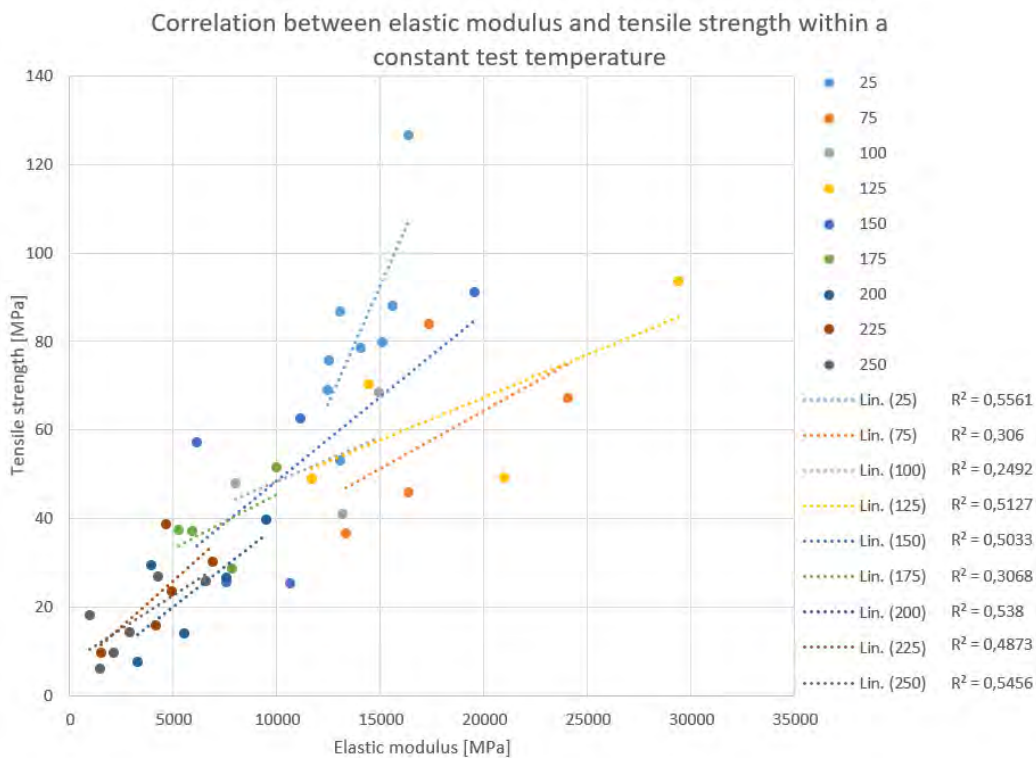


Figure 3.25: The correlation between the modulus of elasticity and the tensile strength

Chapter 4

Simulation model

4.1 Motivation and overview

Based on the literature study and the test results of previous chapters, we can now establish a connection between the rise of temperature in wood, and its tensile strength. In order to use this in practice, as a part of fire safety design, this should be linked to real life scenarios. In the field of fire safety, FDS is often used to simulate the fire and the spreading of smoke. As it also calculates heat transfer to and within objects, it can be used to help establish this connection. Once a fire is simulated in FDS, all we need to do is to obtain the temperature profile within an object of interest, at a plane we deem to be critical. Once this time dependent profile is obtained, it can be compared with either the experimental results of this work, the Eurocode, or user defined data which links the temperature to the remaining strength of the material.

In order to reach this objective, I developed a simple two-part python program. The first part of the program will generate the temperature measuring points to the key locations defined by the user. Next step is to add these to the FDS-model and run the simulation normally. The second part of the program reads the FDS output data and gives the user the time development of the strength, both as data and figure. This can be then used to analyze the performance and duration of the structure in the fire. The option of using the temperature-strength relations presented in Eurocode 5 Annex B provides the designer with tools that are accepted in the Eurocode. A careful and precise definition of the material properties in FDS will be very critical in order to get even somewhat reliable results. The heat transfer calculation within the material in the FDS simulation may not be at a desired accuracy yet, but future advances in it will make an approach like this even

more relevant and reliable.

As this is only a part of my thesis, the program is still quite rough, and in need of further development. However, it has the potential of becoming a tool that can help fire safety engineers in their work in the years to come.

4.2 Simulation model and FDS

First thing to do in order to make use of the temperature-strength data, either provided by own experiments or Eurocode or other sources, is to create a simulation model. This is most commonly done via FDS, Fire Dynamics Simulator. In this thesis, version 6.6.0 of FDS was used. FDS has been comprehensively validated and verified, thus it is a reliable tool for modeling most common fire scenarios. It is a Computational Fluid Dynamics (CFD) model, developed for the simulation of fires. It solves numerically a form of Navier-Stokes -equations for thermally- or fire-driven flow of fluid. It is appropriate for low Mach-number ($Ma < 0.3$).

In the simulation model, the obstruction of interest is modeled using material parameters of wood, more precisely spruce. The material properties in the pyrolysis model that is used here, are based on cone calorimeter experiment results, which are often used as a tool fire defining fire safety. Eventhough wood consists of cellulose, hemicellulose and lignin, it is here modeled as one substance, in which the material properties of the previously mentioned components are a combination of.

4.3 Python

4.3.1 Overview

Python is an interpreted high-level programming language that was created by Guido van Rossum. It was first released in 1991, and has been frequently updated ever since. In this thesis, Python 3.6.4 was used. In order to make the interface more user-friendly, I decided to craft it using Tkinter, which is Python's standard GUI package. [16] Python was chosen for the software development part of this thesis because of its easy use and understandability. The program developed with Python is divided into two individual entities. The first part, in which measure points are created to the key locations based on the user's consideration and inputs, is from now on referred to as "Key locations". The second part, which collects data from the simulation and interprets it based on the selected reference data, is from now on referred

to as "Post-processing". The whole software is referred to as "Key locations and Post-processing", or "KP" for short. When the user starts the software, the following window appears. Now, the user can click and choose what he or she wants to do. I also included a brief explanation, on what each of the main sides of the software do.

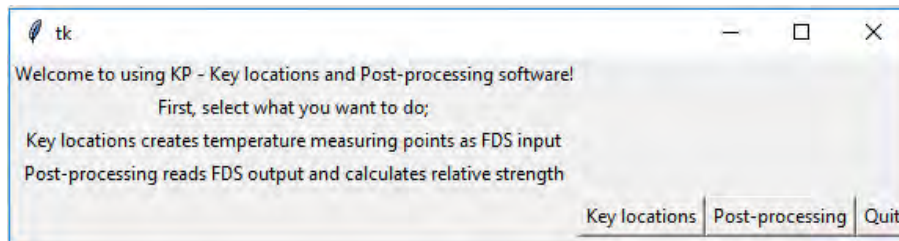


Figure 4.1: First window of KP.

4.3.2 Key locations

If 'Key locations' is selected, the following window appears:

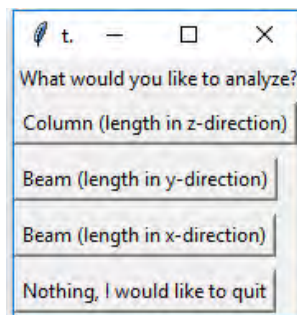


Figure 4.2: First window of Key locations.

Here, the user will choose depending on their FDS geometry, what kind of obstruction they are interested in getting the temperature profile of. This is done in order to define which part of the code is to be used, because depending on the selection, the section to be analyzed is differentially oriented. After the selection, one of the following windows will appear:

Now, based on their FDS geometry, the user fills the blank spaces, and clicks on 'Generate FDS-input'. This will trigger two loops, within which a text file is written. This text file consists of lines which work as measuring

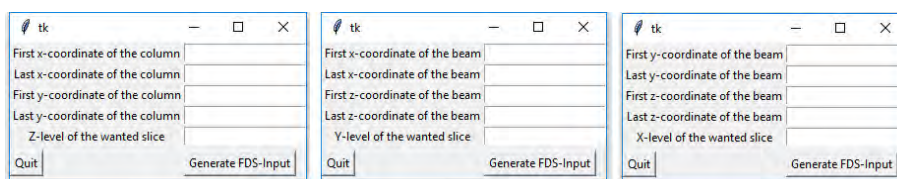


Figure 4.3: Second window of Key locations.

devices inside the FDS code. The quantity that they measure is 'inside wall temperature'. These devices are created on the selected section, with depth varying from front surface to back surface in intervals of 1 mm, and from left surface, to 1 mm below the right surface, with matching interval. The reason that the measuring devices do not reach both of the surfaces in the latter case, is that FDS could not assign them to the correct locations. Now on the selected surface, there are temperature measuring devices every one millimeter, as many as there can be. Now the contents of the text file is manually copied into the FDS script, and the simulation is run.

4.3.3 Post-processing

After the simulation is run, it is time to start the post-processing of data. First it is good to check the device output file with Excel, and if the values are not separated into their own columns, this should be done manually.

After starting the KP software and clicking on 'Post-processing', the following window will appear:

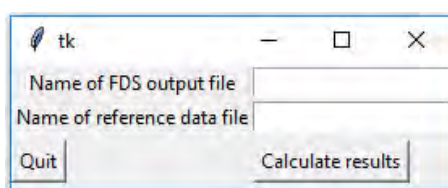


Figure 4.4: First window of Post-processing.

In the fields, the user fills the name of the FDS output file which contains the data from the devices in the simulation (usually named 'simulationname_devc.csv'. Because the software uses csv-reader (Comma separated file), it is important that both the FDS-result file, and the reference data file are saved as .csv, and that the '.csv' is also included in the fields the user fills. When the user clicks 'Calculate results', the software starts its calculations.

First, the software goes through the data contained in the FDS output file. Time is collected from the first column of the file. Then for each row, which is data of the same time step, all the temperatures are collected. Then, the comparison data is accessed to retrieve a relative strength coefficient at each of the temperatures (temperatures are rounded up to an integer to be on the safe side). Next, the coefficients for this timestep are averaged, and thus a relative strength coefficient for the whole obstruction at a certain time is obtained. This process is repeated for all the time steps throughout the simulation. Now, we have a temperature dependent decreased relative strength coefficient as a function of time, which is both plotted to the screen for the user to see, and also written in a text file, titled 'Results.txt'.

4.4 Example case

In order to demonstrate the functioning of the software developed, I created a small FDS model with a 2 m by 6 m by 2 m room. The room has a door in one end in order to give the burning reaction a sufficient amount of oxygen. On the other end of the room, there is a gasoline pool fire. The pool is modeled as a small square, with an area corresponding to a circular pool with radius of only 25 cm, so it resembles a typical container. Above this fire there is a 4 cm by 4 cm wooden beam near the ceiling of the room. The relatively small dimensions of it were chosen in order to speed up the simulation process. This beam is modeled using the material properties of spruce, presented by Mikkola in one of his papers on the subject[14].

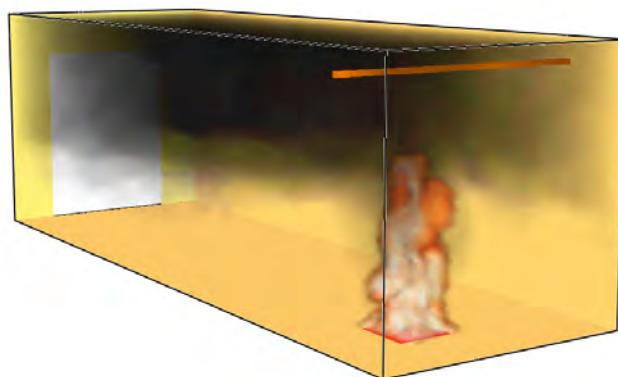


Figure 4.5: Geometry of the simulation model.

The heat release rate of this pool is derived based on the calculation method for burning liquid pools and the thermochemical and empirical constants for gasoline, presented by Hietaniemi in his paper [8].

Maximum burning rate:

$$\dot{m}_{b,max}'' = \dot{m}_{\infty}'' \cdot (1 - \exp(-k_{\beta} \cdot D)) \quad (4.1)$$

Maximum heat release rate of the fire:

$$\dot{Q}_{b,max} = \Delta H_{c,eff} \cdot A_L \cdot \dot{m}_{b,max}'' \quad (4.2)$$

And the time the fire burns:

$$\Delta t = \frac{\rho_L \cdot H_L}{\dot{m}_{b,max}''} \quad (4.3)$$

where $\dot{m}_{b,max}''$ is the maximum mass loss rate [$kgm^{-2}s^{-1}$], \dot{m}_{∞}'' is the asymptotic mass loss rate [$kgm^{-2}s^{-1}$], k_{β} is an empirical constant [m^{-1}], D is the diameter of the pool [m], $\dot{Q}_{b,max}$ is the maximum heat release rate [kW], $\Delta H_{c,eff}$ is the heat of combustion [kJ/kg], A_L is the area of the pool [m^2], t_b is the growth time of the fire [s], g is the gravitational acceleration [m/s^2], ρ_L is the density of the burning liquid [kg/m^3], and Δt is the burning time at maximum burning rate [s].

By placing the given and selected properties for gasoline into the equations 4.1, 4.2 and 4.3 above, we get the following properties for the pool fire:

$$\dot{m}_{b,max}'' = 0,055kgm^{-2}s^{-1} \cdot (1 - \exp(-2,1m^{-1} \cdot 0,5m)) \approx 0,036kgm^{-2}s^{-1}$$

$$\dot{Q}_{b,max} = 43700kJ/kg \cdot 0,196m^2 \cdot 0,036kgm^{-2}s^{-1} \approx 307kW$$

$$\Delta t = \frac{740kg/m^3 \cdot 0,25m}{0,036kgm^{-2}s^{-1}} \approx 5270s$$

The computational domain consists of two meshes; one outer mesh used to calculate the dynamics of the fire and space, and an inner mesh, used mainly to attach the necessary measuring points into the wooden beam.

The grid spacing of the coarser main mesh is based upon the characteristic fire diameter, D^* , which is defined as [13]:

$$D^* = \left(\frac{\dot{Q}}{\rho_\infty c_p T_\infty \sqrt{g}} \right)^{2/5} \quad (4.4)$$

where \dot{Q} is the HRR [kW], ρ_∞ is the density of air [kg/m^3], c_p is the thermal capacity of air, [$kJkg^{-1}K^{-1}$], T_∞ is the ambient temperature [K] and g is the nominal gravitational acceleration [m/s^2].

And in this case, the characteristic fire diameter is:

$$D^* = \left(\frac{307kW}{1,2kg/m^3 \cdot 1kJkg^{-1}K^{-1} \cdot 293K \cdot \sqrt{9,81m/s^2}} \right)^{2/5} \approx 0,60m$$

The ratio between the characteristic fire diameter, D^* and the size of the grid cell δx defines how many computational cells span over the characteristic diameter of fire. It should be noted, that the characteristic diameter of fire does not necessarily equal the physical diameter of fire. The bigger this ratio is, the finer the grid is, resulting in more accurate resolution of the calculation, but also in increased computational time. As a rule of thumb, a ratio of $D^*/\delta x$ between 5 and 10 provides fair results with reasonable computational time. However, the optimal ratio is very case-dependent, and should always be carefully considered. As an example, a validation study on the mesh resolution for NUREG-1824 provided adequate results in calculating the dynamics of the fire plume, at $D^*/\delta x$ ratios between 4 and 16 [20]. In this case, 4 cm was used for δx , resulting in

$$\frac{D^*}{\delta x} = \frac{0,60m}{0,04m} = 15 \quad (4.5)$$

which is deemed appropriate for the situation. The finer grid consists of one of these 4 cm x 4 cm x 4 cm blocks being divided to a 1 mm x 1 mm x 1 mm grid. The finer grid is included to the model in order to be able to fix the measuring devices to the surface of the beam at 1 mm distances from another. Thus, eventhough using a fairly fine mesh as the main computational grid, having to divide only a small block into 1 mm³ pieces saves computational power.

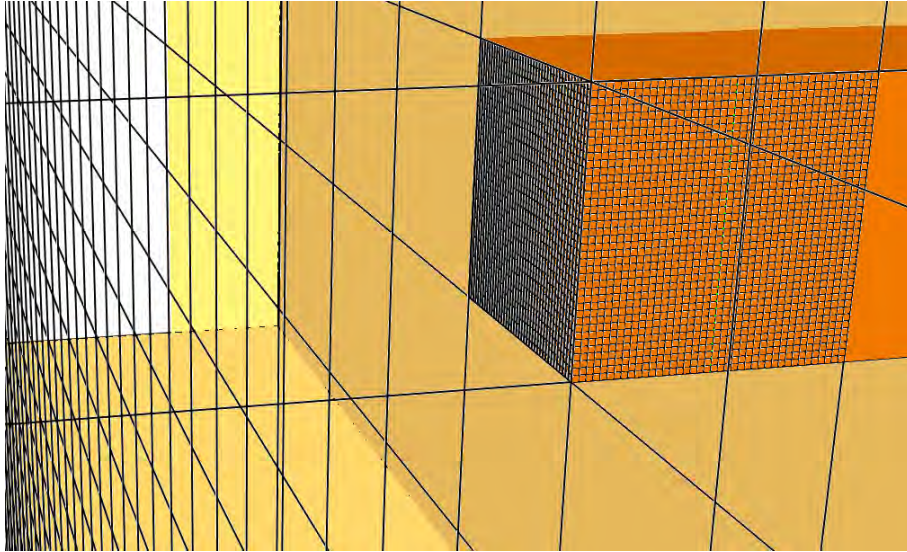


Figure 4.6: Clipped view of the alignments of the coarse mesh and fine mesh within it.

Once the FDS model is ready, the Python program 'KP' introduced in Chapter 4.3 is used to create an FDS input file of the necessary measuring devices to keep tabs on the temperature development inside a section of the wooden beam. After copying the input into the FDS-file, the simulation is run. Then, the post-processing part of 'KP' is used to analyze the results.

Because the current version of FDS uses 1D heat conduction model, the utilization of the finer grid is not yet relevant. The parallel devices which will be created for the model, measuring the temperature at certain depths, produce exactly the same results because of the 1D heat conduction model within the obstacle. The surfaces of the obstacle all work independently, thus having no effect on one another. In future as 3D heat conduction will be included in FDS and the points within the obstacle are influenced by all surfaces, measuring techniques and fine 3D grids such as suggested in this thesis might become useful. Eventhough the result data presented in this chapter comes only from a 1D heat conduction calculation, it can still be used in demonstrating the difference between using the values presented in the Eurocode and the data gathered from experiments as a reference for the analysis. The figure below shows the relative tensional strength derived based on both.

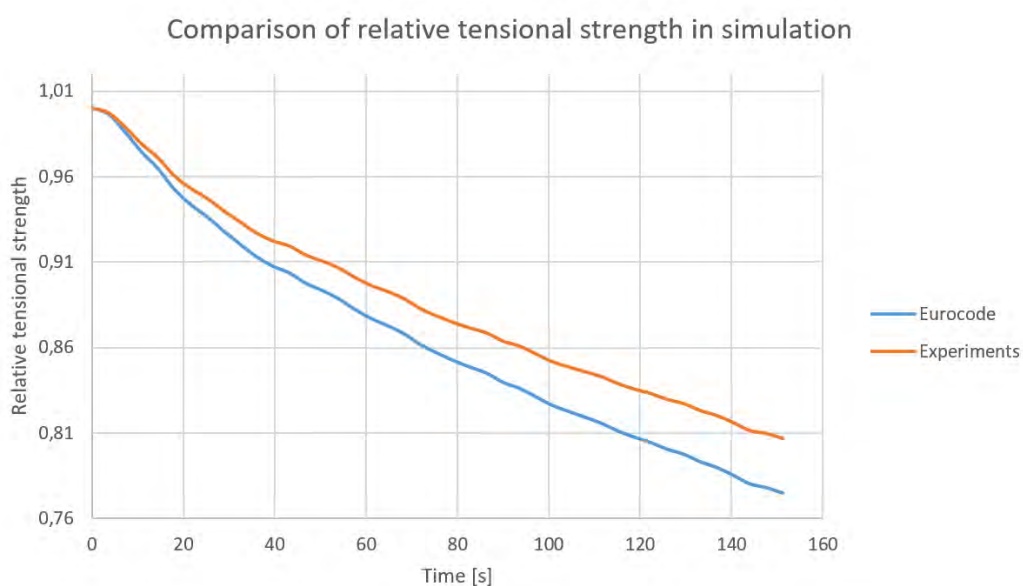


Figure 4.7: Results of the simulation based on the relationship between relative tensional strength and temperature.

By comparing these two, it can be observed that the interpretation based on the Eurocode is on the safe side, as it states that a certain decreased value of the relative tensional strength is reached earlier than in the interpretation based on the experiments I conducted. Also, as time progresses the differentiation between the two curves presented grows larger. This indicates that the wooden beam starts to heat up from the inside too, as the biggest separation between the experimental data and the Eurocode were found near 100 °C. The simulation was only run for 152 seconds due to its massive CPU usage and slow advancement. However, it is already adequate for demonstrative purposes within this thesis.

4.5 Limitations

Because the spacing between measuring points is only 1 mm, this results in very large output files. According to Microsoft, Microsoft Excel has a limit in characters it can fit to one cell. This limit is 32 767 characters. Because some combinations of versions of MS Excel and FDS don't automatically split the rows in cells but this has to be done manually, the limit of 32 767 characters per cell is easily reached, and for example in a simulation with the measuring points spread out to 5 cm x 5 cm area will already cause problems. However, with combination of systems that automatically divide the result files to columns, the current limit with MS Excel (Versions 2016 and 2013) is 16 384 columns, meaning an area of 16 384 mm² (Or 12,8 cm x 12,8 cm). If the obstruction we want to analyze is larger, this problem can be easily dealt with by changing the python code to creating a measuring point grid with distances larger than 1 mm. However, the more scarce the measuring points are located, the less accurate the overall results will be. For this reason, I did not initially include a changing of the spacing option in to the software's graphical user interface.

The current version of FDS uses 1D heat conduction. This means, that by the utilization of the finer grid and the multiple parallel measuring points, no additional value is gained. However, as the 3D heat conduction models advance and become common practice, this approach could become widely used. Before this can be done, it has to be properly tested, adjusted and evaluated. The model and software presented within this thesis thus work only as a prototype that can be exploited in the future. Because the heat conduction in the model is only calculated in 1D, it can not be used to determine the realistic temperature profile within the object.

The measuring points created are now all in one plane, which has to be predetermined. In the future, the temperature profile could be acquired for the whole beam. This would mean, that the section under observation could be chosen after the simulation is run. Also, a graphical representation of the temperature profile could be created. With this, the user could see the advancement of the charring front, as well as the heat profile within the object at desired times.

The material model within FDS is an approximation at best, and especially for wood, the simulation and real-life behaviour and properties may vary. This should be taken into account when using this type of analysis, and the results should not be applied to design purposes without thorough consideration and critical thinking.

The FDS script should only contain the devices made by the software,

meaning that other measurements should not be added by the user. This is because the software goes through them all without separating which is which. In the case of a averaged strength profile through time, the location of the devices does not matter, as the loading is assumed to be homogenous. In a real-life scenario however, this is rarely the case. This is one of the aspects of the software that could be further developed in the future. For example combining the individual point data of the temperature, to a model which contains the direction and magnitude of the stress at the same point would provide very useful data on structural analysis during fires.

Chapter 5

Conclusions

The literature study presented in chapter 2 demonstrates the fact, that wood is a living material with high variation in its properties. Although its strength properties in high temperature have been studied to some extent, more focus should be directed to the subject. As the data gathered by different researchers varies quite a bit, it is difficult to know which data describes the effect of temperature on the tensile strength of wood most accurately, and is the best for real-world applications.

In order to produce scientifically accurate and significant data, the methods used in collecting and evaluating it have to be adequate, and uncertainty has to be addressed accordingly. In the experiments conducted within this thesis, these methods fall a bit short due to the circumstances. Eventhough the data gathered on the tensile strength of the samples shows clear correlation with the data presented in the eurocode, the amount of samples is too little to make reliable and accurate statements.

As a further improvement to the experiment setting, strain data could be collected on both sides of the samples, which was now not possible due to the restricting geometry of the furnace used. Also, conducting studies to demonstrate whether or not the time the sample stays in elevated temperature has any effect on its elastic and strength properties should be conducted, while measuring the strain caused by shrinking due to loss of moisture and thermal expansion.

Overall, the experiments conducted within this thesis correlate well with the relationship between tensile strength and temperature presented in the Eurocode EN 1995-1-2. This is a good thing, indicating that using the methods presented within the Eurocode are in line with reality and will not cause dangerous design decisions, provided that they are used correctly.

Eventhough the post processing of the simulation model presented in this thesis is mainly a vision of the future as it would require 3D heat conduction model, the results of the tensile strength experiment can be utilized also with current simulation technology. This could be done e.g. by keeping tabs on the temperature development of each side of the object, and by using the known heat conduction properties within wood, calculating the temperature profile by hand. However this would still be only an approximation, and very time consuming.

The simulation of fires is gaining more and more ground among the fire safety engineering community as the tool for proving buildings-to-be safe, so further research should be directed towards material properties under exposure to elevated temperatures. For wood, this could be done by continuing along the same testing principles presented and evaluated in this thesis. By making use of the data gathered, more effective tools for engineering could be developed, leading the whole building industry to a brighter future.

Bibliography

- [1] ATREYA, A. Pyrolysis, Ignition and Fire Spread on Horizontal Surfaces of Wood. *Ph. D. Thesis* (1983).
- [2] B.A.-L. ÖSTMAN. Wood tensile strength at temperatures and moisture contents simulating fire conditions, 1985.
- [3] CEN. Eurocode 5: Design of timber structures - part 1-2: General structural fire design, 2004.
- [4] DRYSDALE, D. An introduction to fire dynamics. 3rd edition, 2007.
- [5] FOREST PRODUCTS LIBRARY. Wood handbook, wood as an engineering material, 2010.
- [6] FREDLUND, B. Modelling of Heat and Mass Transfer in Wood Structures During Fire. *Fire Safety Journal* 20 (1993), 39–69.
- [7] GALGANO, A. AND DI BLASI, C. Modeling wood degradation by the unreacted-core-shrinking approximation. *Industrial & Engineering Chemistry Research* 42 (2003), 2101–2111.
- [8] HIETANIEMI, J. Palon voimakkuuden kuvaaminen toiminnallisessa paloteknisessä suunnittelussa, 2007.
- [9] KOLLMAN, F., COTE, W. Principles of wood science and technology I, 1968.
- [10] KÖNIG, J. Timber frame assemblies exposed to standard and parametric fires., 2000.
- [11] LIU, W.-T., TSAI, M.-T., AND FITRIANA, L. Experimental study on residual compressive strength of bamboo column under fire with different time limitation. *World Conference on Timber Engineering 2016* (2016), 5235–5242. <https://owncloud.tuwien.ac.at/index.php/s/eoBaUfyBgtDsvYC#pdfviewer>. Accessed 18.1.2018.

- [12] MAKU, T. Studies on the heat conduction in wood. *Bulletin of the Wood Research Institute, No 13* (1954).
- [13] MCGRATTAN, K., HOSTIKKA, S., MCDERMOTT, R., FLOYD, J., VANELLA, M., WEINSCHENK, C., OVERHOLT, K. Fire dynamics simulator user's guide, 2017.
- [14] MIKKOLA, E. Puupinnan syttyminen. *VTT Tiedotteita 1057* (1989), 48 s.
- [15] PARKER, W. J. Development of a model for the heat release of wood - A status report, 1985.
- [16] PYTHON SOFTWARE FOUNDATION. Python's official websites. webpage. <https://www.python.org/>. Accessed 11.4.2018.
- [17] RANTA-MAUNUS, A. The Viscoelasticity of Wood at Varying Moisture Content. *Wood Science and Technology, Vol. 9* (1975), 189–205.
- [18] REGUEIRA, R.; LINARES, V.; LAGANA, R.; GUAITA, M. Modeling of variation in the mechanical properties of beechwood at elevated temperatures using finite element method. *World Conference on Timber Engineering 2016* (2016), 2626–2634. <https://owncloud.tuwien.ac.at/index.php/s/eoBaUfyBgtDsvYC#pdfviewer>. Accessed 18.1.2018.
- [19] SCHMID, J., ET ALL. The Reduced Cross-Section Method for Evaluation of the Fire Resistance of Timber Members: Discussion and Determination of the Zero-Strength Layer. *Fire Technology, 51* (2015), 1285–1309.
- [20] U.S. NUCLEAR REGULATORY COMMISSION. Verification and validation of selected fire models for nuclear power plant applications. volume 7: Fire dynamics simulator (fds), 2010. <https://www.nrc.gov/docs/ML0717/ML071730543.pdf>. Accessed 5.6.2018.
- [21] YMPÄRISTÖMINISTERIÖ. Ympäristöministeriön asetus rakennusten paloturvallisuudesta, 2017. <https://www.finlex.fi/fi/laki/alkup/2017/20170848>. Accessed 22.10.2018.

Appendix A

FDS Scripts

Sample in oven

```
&HEAD CHID='Spruce_simple_cone',TITLE='standard cone calorimeter' /
&MESH IJK=3,3,4
XB = -0.15,0.15,-0.15,0.15,-0.1,0.3 /

&TIME T_END=1000., DT = 0.5, WALL_INCREMENT = 1 / 600

&RADI NUMBER_RADIATION_ANGLES= 100 /
&DUMP DT_PL3D = 10000000./STATUS_FILES = .TRUE. /SMOKE3D = .FALSE. /

&VENT XB = -0.05,0.05,-0.05,0.05,-0.1,-0.1, SURF_ID = 'SPRUCE' /

&SURF ID = 'SPRUCE'
RGB =200,100,0
THICKNESS = 0.0035
MATL_ID = 'SPRUCE'
BACKING = 'INSULATED'
MINIMUM_LAYER_THICKNESS = 1E-10 /

MATL ID = 'WATER'
EMISSIVITY = 1.0
DENSITY = 1000.
CONDUCTIVITY = 0.016
SPECIFIC_HEAT = 4.3
N_REACTIONS = 1
A = 9.5712677e+22
E = 135663.11
N_S = 3.3119154
NU_SPEC = 1
SPEC_ID = 'WATER VAPOR'
HEAT_OF_REACTION = 0/

&MATL ID = 'SPRUCE'
EMISSIVITY = 1.0
DENSITY = 440.
CONDUCTIVITY_RAMP = 'RAMP_Spruce_K',
SPECIFIC_HEAT_RAMP = 'RAMP_Spruce_C',
N_REACTIONS = 1
A = 5.58E7
```



```

E = 1.23E5
N_S = 1
NU_SPEC = 0.8356
NU_MATL = 0.1644
SPEC_ID = 'PROPANE'
MATL_ID = 'CHAR'
HEAT_OF_REACTION = 300.
HEAT_OF_COMBUSTION = 13100. /

/Mikkola, E. 1989. Puupinnan syttyminen

&RAMP ID = 'RAMP_Spruce_K', T = 20, F = 0.125 /
&RAMP ID = 'RAMP_Spruce_K', T = 360, F = 0.163 /

/Dunlap

&RAMP ID = 'RAMP_Spruce_C', T = 20, F = 1.21 /
&RAMP ID = 'RAMP_Spruce_C', T = 300, F = 2.58 /

&MATL ID = 'CHAR'
EMISSIVITY = 1
DENSITY = 101.
CONDUCTIVITY = 0.55
SPECIFIC_HEAT = 2.5 /

&REAC ID = 'PROPANE'
      FUEL = 'PROPANE'
SOOT_YIELD = 0.01
C = 3
H = 8
HEAT_OF_COMBUSTION = 46450.
IDEAL = .TRUE. /

&SPEC ID = 'WATER VAPOR' /
(Rath USA)
MATL ID          = 'CASI'
      EMISSIVITY      = 1.0
      CONDUCTIVITY_RAMP = 'RAMP_K'
      DENSITY         = 250.
      SPECIFIC_HEAT   = 0.92 /
RAMP ID = 'RAMP_K', T = 100, F = 0.065 /
RAMP ID = 'RAMP_K', T = 800, F = 0.11 /

&MATL ID          = 'WOOL'
      EMISSIVITY      = 1.0
      CONDUCTIVITY_RAMP = 'RAMP_K'
      DENSITY         = 64.
      SPECIFIC_HEAT   = 0.7 /
&RAMP ID = 'RAMP_K', T = 260, F = 0.08 /
&RAMP ID = 'RAMP_K', T = 538, F = 0.19 /
&RAMP ID = 'RAMP_K', T = 816, F = 0.36 /

&SURF ID = 'HOT' TMP_FRONT = 75. RAMP_T = 'OMA' DEFAULT = .TRUE. /
&RAMP ID = 'OMA' T = 0, F = 1.0 /
&RAMP ID = 'OMA' T = 3600, F = 1.0 /

&DEVC ID='Oven temp', XYZ=0,0,0, QUANTITY='TEMPERATURE' /

```

```
&DEVC XYZ=0,0,-0.1, QUANTITY='INSIDE WALL TEMPERATURE', DEPTH=0.0000001, ID='Temp_0mm', IOR=3 /
&DEVC XYZ=0,0,-0.1, QUANTITY='INSIDE WALL TEMPERATURE', DEPTH=0.001, ID='Temp_1mm', IOR=3 /
&DEVC XYZ=0,0,-0.1, QUANTITY='INSIDE WALL TEMPERATURE', DEPTH=0.002, ID='Temp_2mm', IOR=3 /
&DEVC XYZ=0,0,-0.1, QUANTITY='INSIDE WALL TEMPERATURE', DEPTH=0.003, ID='Temp_3mm', IOR=3 /
&DEVC XYZ=0,0,-0.1, QUANTITY='INSIDE WALL TEMPERATURE', DEPTH=0.00349, ID='Temp_3.5mm', IOR=3 /
```

```
&BNDF QUANTITY = 'WALL TEMPERATURE' /
&TAIL /
```

Simulation with wooden beam

```
Palotilabeam.fds
Generated by PyroSim - Version 2017.2.1115
29.3.2018 14:50:27
```

```
&HEAD CHID='181101Palotilabeamx'/
&TIME T_END=3600.0/
&DUMP RENDER_FILE='18101Palotilabeamx.ge1', DT_RESTART=300.0, DT_SL3D=0.25/
```

```
&MESH ID='MESH', IJK=50,150,50, XB=0.0,2.0,0.0,6.0,0.0,2.0/
&MESH ID='MESH01', IJK=40,40,40, XB=0.72,0.76,0.52,0.56,1.8,1.84/
```

```
&SURF ID = 'SPRUCE'
      RGB =200,100,0
      MATL_ID='SPRUCE'
      BACKING = 'EXPOSED'
      THICKNESS = 0.04
```

```
&MATL ID = 'SPRUCE'
EMISSION = 1.0
DENSITY = 440.
CONDUCTIVITY_RAMP = 'RAMP_Spruce_K',
SPECIFIC_HEAT_RAMP = 'RAMP_Spruce_C',
N_REACTIONS = 1
A = 5.58E7
E = 1.23E5
N_S = 1
NU_SPEC = 0.8356
NU_MATL = 0.1644
SPEC_ID = 'PROPANE'
MATL_ID = 'CHAR'
HEAT_OF_REACTION = 300.
HEAT_OF_COMBUSTION = 13100. /
```

```
/Mikkola, E. 1989. Puupinnan syttyminen
```

```
&RAMP ID = 'RAMP_Spruce_K', T = 20, F = 0.125 /
&RAMP ID = 'RAMP_Spruce_K', T = 360, F = 0.163 /
```

```
/Dunlap
```

APPENDIX A. FDS SCRIPTS

67

```
&RAMP ID = 'RAMP_Spruce_C', T = 20, F = 1.21 /
&RAMP ID = 'RAMP_Spruce_C', T = 300, F = 2.58 /

&MATL ID = 'CHAR'
EMISSIVITY = 1
DENSITY = 101.
CONDUCTIVITY = 0.55
SPECIFIC_HEAT = 2.5 /

&REAC ID = 'PROPANE'
FUEL = 'PROPANE'
SOOT_YIELD = 0.01
C = 3
H = 8
HEAT_OF_COMBUSTION = 46450.
IDEAL = .TRUE. /

&SURF ID='FIRE',
COLOR='RED',
HRRPUA=1585.0/

&OBST ID='Obstruction', XB=0.0,2.0,0.52,0.56,1.8,1.84, SURF_ID='SPRUCE'/

&VENT ID='FIREVENT', SURF_ID='FIRE', XB=0.56,1.0,0.56,1.0,0.0,0.0/
&VENT ID='Vent', SURF_ID='OPEN', XB=0.4,1.6,6.0,6.0,0.0,1.6/
&DEVC XYZ= 0.74 , 0.52 , 1.8 , QUANTITY='INSIDE WALL TEMPERATURE', DEPTH= 0.0 , ID=' 0.0 0 mm', IOR=-2 /
&DEVC XYZ= 0.74 , 0.52 , 1.8 , QUANTITY='INSIDE WALL TEMPERATURE', DEPTH= 0.001 , ID=' 0.0 1 mm', IOR=-2 /
&DEVC XYZ= 0.74 , 0.52 , 1.8 , QUANTITY='INSIDE WALL TEMPERATURE', DEPTH= 0.002 , ID=' 0.0 2 mm', IOR=-2 /
&DEVC XYZ= 0.74 , 0.52 , 1.8 , QUANTITY='INSIDE WALL TEMPERATURE', DEPTH= 0.003 , ID=' 0.0 3 mm', IOR=-2 /
&DEVC XYZ= 0.74 , 0.52 , 1.8 , QUANTITY='INSIDE WALL TEMPERATURE', DEPTH= 0.004 , ID=' 0.0 4 mm', IOR=-2 /
&DEVC XYZ= 0.74 , 0.52 , 1.8 , QUANTITY='INSIDE WALL TEMPERATURE', DEPTH= 0.005 , ID=' 0.0 5 mm', IOR=-2 /
&DEVC XYZ= 0.74 , 0.52 , 1.8 , QUANTITY='INSIDE WALL TEMPERATURE', DEPTH= 0.006 , ID=' 0.0 6 mm', IOR=-2 /
&DEVC XYZ= 0.74 , 0.52 , 1.8 , QUANTITY='INSIDE WALL TEMPERATURE', DEPTH= 0.007 , ID=' 0.0 7 mm', IOR=-2 /
&DEVC XYZ= 0.74 , 0.52 , 1.8 , QUANTITY='INSIDE WALL TEMPERATURE', DEPTH= 0.008 , ID=' 0.0 8 mm', IOR=-2 /
&DEVC XYZ= 0.74 , 0.52 , 1.8 , QUANTITY='INSIDE WALL TEMPERATURE', DEPTH= 0.009 , ID=' 0.0 9 mm', IOR=-2 /
&DEVC XYZ= 0.74 , 0.52 , 1.8 , QUANTITY='INSIDE WALL TEMPERATURE', DEPTH= 0.01 , ID=' 0.0 10 mm', IOR=-2 /
&DEVC XYZ= 0.74 , 0.52 , 1.8 , QUANTITY='INSIDE WALL TEMPERATURE', DEPTH= 0.011 , ID=' 0.0 11 mm', IOR=-2 /
&DEVC XYZ= 0.74 , 0.52 , 1.8 , QUANTITY='INSIDE WALL TEMPERATURE', DEPTH= 0.012 , ID=' 0.0 12 mm', IOR=-2 /
&DEVC XYZ= 0.74 , 0.52 , 1.8 , QUANTITY='INSIDE WALL TEMPERATURE', DEPTH= 0.013 , ID=' 0.0 13 mm', IOR=-2 /
&DEVC XYZ= 0.74 , 0.52 , 1.8 , QUANTITY='INSIDE WALL TEMPERATURE', DEPTH= 0.014 , ID=' 0.0 14 mm', IOR=-2 /
&DEVC XYZ= 0.74 , 0.52 , 1.8 , QUANTITY='INSIDE WALL TEMPERATURE', DEPTH= 0.015 , ID=' 0.0 15 mm', IOR=-2 /
&DEVC XYZ= 0.74 , 0.52 , 1.8 , QUANTITY='INSIDE WALL TEMPERATURE', DEPTH= 0.016 , ID=' 0.0 16 mm', IOR=-2 /
&DEVC XYZ= 0.74 , 0.52 , 1.8 , QUANTITY='INSIDE WALL TEMPERATURE', DEPTH= 0.017 , ID=' 0.0 17 mm', IOR=-2 /
&DEVC XYZ= 0.74 , 0.52 , 1.8 , QUANTITY='INSIDE WALL TEMPERATURE', DEPTH= 0.018 , ID=' 0.0 18 mm', IOR=-2 /
&DEVC XYZ= 0.74 , 0.52 , 1.8 , QUANTITY='INSIDE WALL TEMPERATURE', DEPTH= 0.019 , ID=' 0.0 19 mm', IOR=-2 /
&DEVC XYZ= 0.74 , 0.52 , 1.8 , QUANTITY='INSIDE WALL TEMPERATURE', DEPTH= 0.02 , ID=' 0.0 20 mm', IOR=-2 /
&DEVC XYZ= 0.74 , 0.52 , 1.8 , QUANTITY='INSIDE WALL TEMPERATURE', DEPTH= 0.021 , ID=' 0.0 21 mm', IOR=-2 /
&DEVC XYZ= 0.74 , 0.52 , 1.8 , QUANTITY='INSIDE WALL TEMPERATURE', DEPTH= 0.022 , ID=' 0.0 22 mm', IOR=-2 /
&DEVC XYZ= 0.74 , 0.52 , 1.8 , QUANTITY='INSIDE WALL TEMPERATURE', DEPTH= 0.023 , ID=' 0.0 23 mm', IOR=-2 /
&DEVC XYZ= 0.74 , 0.52 , 1.8 , QUANTITY='INSIDE WALL TEMPERATURE', DEPTH= 0.024 , ID=' 0.0 24 mm', IOR=-2 /
&DEVC XYZ= 0.74 , 0.52 , 1.8 , QUANTITY='INSIDE WALL TEMPERATURE', DEPTH= 0.025 , ID=' 0.0 25 mm', IOR=-2 /
&DEVC XYZ= 0.74 , 0.52 , 1.8 , QUANTITY='INSIDE WALL TEMPERATURE', DEPTH= 0.026 , ID=' 0.0 26 mm', IOR=-2 /
&DEVC XYZ= 0.74 , 0.52 , 1.8 , QUANTITY='INSIDE WALL TEMPERATURE', DEPTH= 0.027 , ID=' 0.0 27 mm', IOR=-2 /
&DEVC XYZ= 0.74 , 0.52 , 1.8 , QUANTITY='INSIDE WALL TEMPERATURE', DEPTH= 0.028 , ID=' 0.0 28 mm', IOR=-2 /
&DEVC XYZ= 0.74 , 0.52 , 1.8 , QUANTITY='INSIDE WALL TEMPERATURE', DEPTH= 0.029 , ID=' 0.0 29 mm', IOR=-2 /
&DEVC XYZ= 0.74 , 0.52 , 1.8 , QUANTITY='INSIDE WALL TEMPERATURE', DEPTH= 0.03 , ID=' 0.0 30 mm', IOR=-2 /
&DEVC XYZ= 0.74 , 0.52 , 1.8 , QUANTITY='INSIDE WALL TEMPERATURE', DEPTH= 0.031 , ID=' 0.0 31 mm', IOR=-2 /
&DEVC XYZ= 0.74 , 0.52 , 1.8 , QUANTITY='INSIDE WALL TEMPERATURE', DEPTH= 0.032 , ID=' 0.0 32 mm', IOR=-2 /
&DEVC XYZ= 0.74 , 0.52 , 1.8 , QUANTITY='INSIDE WALL TEMPERATURE', DEPTH= 0.033 , ID=' 0.0 33 mm', IOR=-2 /
&DEVC XYZ= 0.74 , 0.52 , 1.8 , QUANTITY='INSIDE WALL TEMPERATURE', DEPTH= 0.034 , ID=' 0.0 34 mm', IOR=-2 /
```


Appendix B

Python Script

KP - Key locations and Post-processing

```
from tkinter import *
import csv
from decimal import *
import matplotlib.pyplot as plt
import math
import numpy as np

getcontext().prec=4

def key_locations():

def beamx_calc():

def save_entry_fields3():
Y_0 = e1.get()
Y_L = e2.get()
Z_0 = e3.get()
Z_L = e4.get()
X = e5.get()
print(Y_0)
print(Y_L)
print(Z_0)
print(Z_L)
print(X)

nro_y=(Decimal(Y_L)-Decimal(Y_0))*1000
nro_z=(Decimal(Z_L)-Decimal(Z_0))*1000

a=[]
j=0
v=10
z=2
```

```

y=3

with open("Input for FDS beam_x.txt", "w") as text_file:
while j < nro_z:
i=0
while i-1 < nro_y:
apu=float(Decimal(Z_0)+Decimal((j/1000)))
print("&DEVC XYZ=",str(X),"",str(Y_0),"",apu,"", QUANTITY='INSIDE WALL TEMPERATURE', DEPTH=",str(i/1000)", ID=',s
i=i+1
j=j+1

master = Tk()
Label(master, text="First y-coordinate of the beam").grid(row=0)
Label(master, text="Last y-coordinate of the beam").grid(row=1)
Label(master, text="First z-coordinate of the beam").grid(row=2)
Label(master, text="Last z-coordinate of the beam").grid(row=3)
Label(master, text="X-level of the wanted slice").grid(row=4)

e1 = Entry(master)
e2 = Entry(master)
e3 = Entry(master)
e4 = Entry(master)
e5 = Entry(master)

e1.grid(row=0, column=1)
e2.grid(row=1, column=1)
e3.grid(row=2, column=1)
e4.grid(row=3, column=1)
e5.grid(row=4, column=1)

Button(master, text='Quit', command=master.quit).grid(row=6, column=0, sticky=W, pady=4)
Button(master, text='Generate FDS-Input', command=save_entry_fields3).grid(row=6, column=1, sticky=W, pady=4)

mainloop( )

def beamy_calc():

def save_entry_fields2():
X_0 = e1.get()
X_L = e2.get()
Z_0 = e3.get()
Z_L = e4.get()
Y = e5.get()
print(X_0)
print(X_L)
print(Z_0)
print(Z_L)
print(Y)

nro_x=(Decimal(X_L)-Decimal(X_0))*1000
nro_z=(Decimal(Z_L)-Decimal(Z_0))*1000

a=[]
j=0
v=10
z=2
x=3

```



```

with open("Input for FDS beam_y.txt", "w") as text_file:
while j < nro_z:
i=0
while i-1 < nro_x:
apu=str(Decimal(Z_0)+Decimal((j/1000)))
print("&DEVC XYZ=",str(X_0),",",str(Y),",",apu,", QUANTITY='INSIDE WALL TEMPERATURE', DEPTH=",str(i/1000),", ID='",s
i=i+1
j=j+1

master = Tk()
Label(master, text="First x-coordinate of the beam").grid(row=0)
Label(master, text="Last x-coordinate of the beam").grid(row=1)
Label(master, text="First z-coordinate of the beam").grid(row=2)
Label(master, text="Last z-coordinate of the beam").grid(row=3)
Label(master, text="Y-level of the wanted slice").grid(row=4)

e1 = Entry(master)
e2 = Entry(master)
e3 = Entry(master)
e4 = Entry(master)
e5 = Entry(master)

e1.grid(row=0, column=1)
e2.grid(row=1, column=1)
e3.grid(row=2, column=1)
e4.grid(row=3, column=1)
e5.grid(row=4, column=1)

Button(master, text='Quit', command=master.quit).grid(row=6, column=0, sticky=W, pady=4)
Button(master, text='Generate FDS-Input', command=save_entry_fields2).grid(row=6, column=1, sticky=W, pady=4)

mainloop( )

def column_calc():

def save_entry_fields1():
X_0 = e1.get()
X_L = e2.get()
Y_0 = e3.get()
Y_L = e4.get()
Z = e5.get()
print(X_0)
print(X_L)
print(Y_0)
print(Y_L)
print(Z)

nro_y=(Decimal(Y_L)-Decimal(Y_0))*1000
nro_x=(Decimal(X_L)-Decimal(X_0))*1000

a=[]
j=0
v=10
x=2
y=3

with open("Input for FDS column.txt", "w") as text_file:
while j < nro_x:
i=0

```

```

while i-1 < nro_y:
apu=str(Decimal(X_0)+Decimal((j/1000)))
print("&DEVC XYZ=",apu,"",str(Y_0),"",str(Z),"", QUANTITY='INSIDE WALL TEMPERATURE', DEPTH=",str(i/1000),"", ID='',s
i=i+1
j=j+1

master = Tk()
Label(master, text="First x-coordinate of the column").grid(row=0)
Label(master, text="Last x-coordinate of the column").grid(row=1)
Label(master, text="First y-coordinate of the column").grid(row=2)
Label(master, text="Last y-coordinate of the column").grid(row=3)
Label(master, text="Z-level of the wanted slice").grid(row=4)

e1 = Entry(master)
e2 = Entry(master)
e3 = Entry(master)
e4 = Entry(master)
e5 = Entry(master)

e1.grid(row=0, column=1)
e2.grid(row=1, column=1)
e3.grid(row=2, column=1)
e4.grid(row=3, column=1)
e5.grid(row=4, column=1)

Button(master, text='Quit', command=master.quit).grid(row=6, column=0, sticky=W, pady=4)
Button(master, text='Generate FDS-Input', command=save_entry_fields1).grid(row=6, column=1, sticky=W, pady=4)

mainloop( )

master = Tk()
Label(master, text="What would you like to analyze?").grid(row=0)

Button(master, text='Nothing, I would like to quit', command=master.quit).grid(row=5, column=0, sticky=W, pady=4)
Button(master, text='Beam (length in x-direction)', command=beamx_calc).grid(row=4, column=0, sticky=W, pady=4)
Button(master, text='Beam (length in y-direction)', command=beamy_calc).grid(row=3, column=0, sticky=W, pady=4)
Button(master, text='Column (length in z-direction)', command=column_calc).grid(row=2, column=0, sticky=W, pady=4)

mainloop( )

def post_processing():

def analyze_results():
fdsfile = []
fdsfile.append(e1.get())
comparisonfile = []
comparisonfile.append(e2.get())
with open(comparisonfile[0]) as f:
reader = csv.reader(f, delimiter=";")
kertoimet= []
for row in reader:
kertoimet.append(row[0])

print(kertoimet)

valmis= []
lampolista= []

```

```
with open(fdsfile[0]) as f:
reader = csv.reader(f, delimiter=";")
ajat= []
i=0
for row in reader:
ajat.append(row[0])
if i>1:
print(row[1:])
lampolista.append(row[1:])
print(len(row))
i=i+1

ajat=ajat[2:]
print(ajat)
print(lampolista)

a=(len(lampolista))
b=(len(lampolista[0]))
print(b)
i=0

apulista=[]

while i<a:
j=0
apulista=[]
while j<b:
print(kertoimet[int(math.ceil(float(lampolista[i][j])))))
apulista.append(float(kertoimet[int(math.ceil(float(lampolista[i][j])))))
j=j+1
print(apulista)
print(sum(apulista)/len(apulista))
valmis.append(sum(apulista)/len(apulista))
print(lampolista[i])
i=i+1

i=0
while i < (len(ajat) ):
ajat[i]=float(ajat[i])
i=i+1
print(valmis)
print(ajat)

if len(ajat) < 20:
ticks = 1
elif len(ajat) < 50:
ticks = 5
elif len(ajat) < 100:
ticks = 10
elif len(ajat) < 200:
ticks = 20
elif len(ajat) < 300:
ticks = 30
elif len(ajat) < 400:
ticks = 40
elif len(ajat) < 500:
ticks = 50
elif len(ajat) < 600:
ticks = 60
elif len(ajat) < 700:
ticks = 70
```

```
elif len(ajat) < 800:
    ticks = 80
elif len(ajat) < 900:
    ticks = 90
else:
    ticks = 100

with open("Results.txt", "w") as text_file:
    print(ajat, valmis, file=text_file)

plt.plot(ajat, valmis)
plt.xticks(np.arange(min(ajat), max(ajat)+1, ticks))
plt.xlabel('Time [s]')
plt.ylabel('Relative strength')

plt.title('Relative strength throughout the simulation')

plt.show()

master = Tk()
Label(master, text="Name of FDS output file").grid(row=0)
Label(master, text="Name of reference data file").grid(row=1)

e1 = Entry(master)
e2 = Entry(master)

e1.grid(row=0, column=1)
e2.grid(row=1, column=1)

Button(master, text='Quit', command=master.quit).grid(row=6, column=0, sticky=W, pady=4)
Button(master, text='Calculate results', command=analyze_results).grid(row=6, column=1, sticky=W, pady=4)

mainloop( )

master = Tk()
Label(master, text="Welcome to using KP - Key locations and Post-processing software!").grid(row=0)
Label(master, text="First, select what you want to do;").grid(row=1, column=0)
Label(master, text="Key locations creates temperature measuring points as FDS input").grid(row=3)
Label(master, text="Post-processing reads FDS output and calculates relative strength").grid(row=4)

Button(master, text='Quit', command=master.quit).grid(row=6, column=3, sticky=W, pady=4)
Button(master, text='Key locations', command=key_locations).grid(row=6, column=1, sticky=W, pady=4)
Button(master, text='Post-processing', command=post_processing).grid(row=6, column=2, sticky=W, pady=4)

mainloop( )
```

Appendix C

Tensile Test Graphs

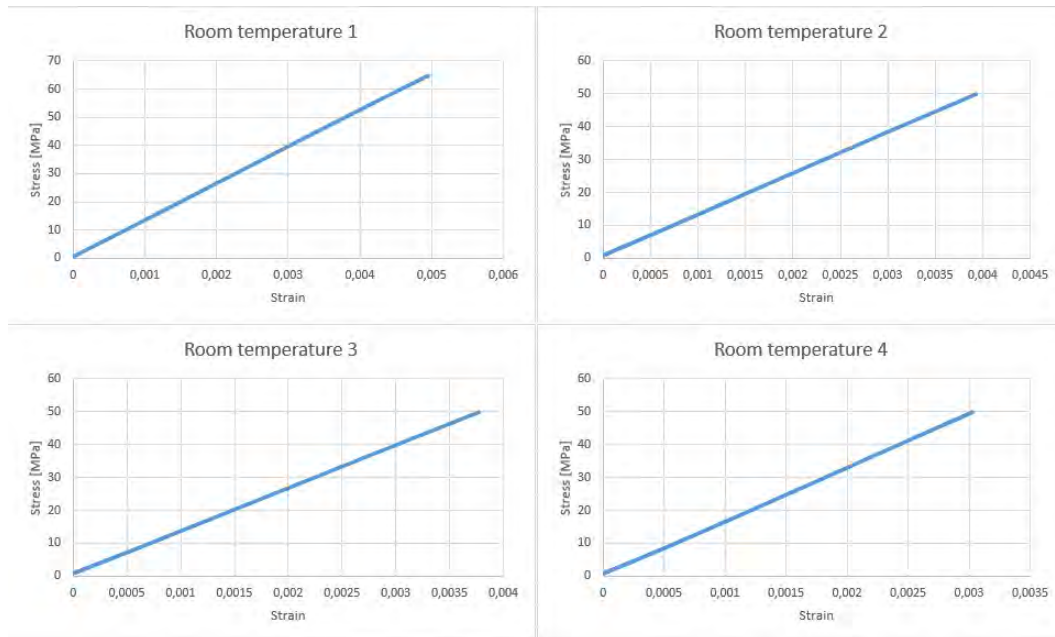


Figure C.1: Strain measured of samples at 25 °C

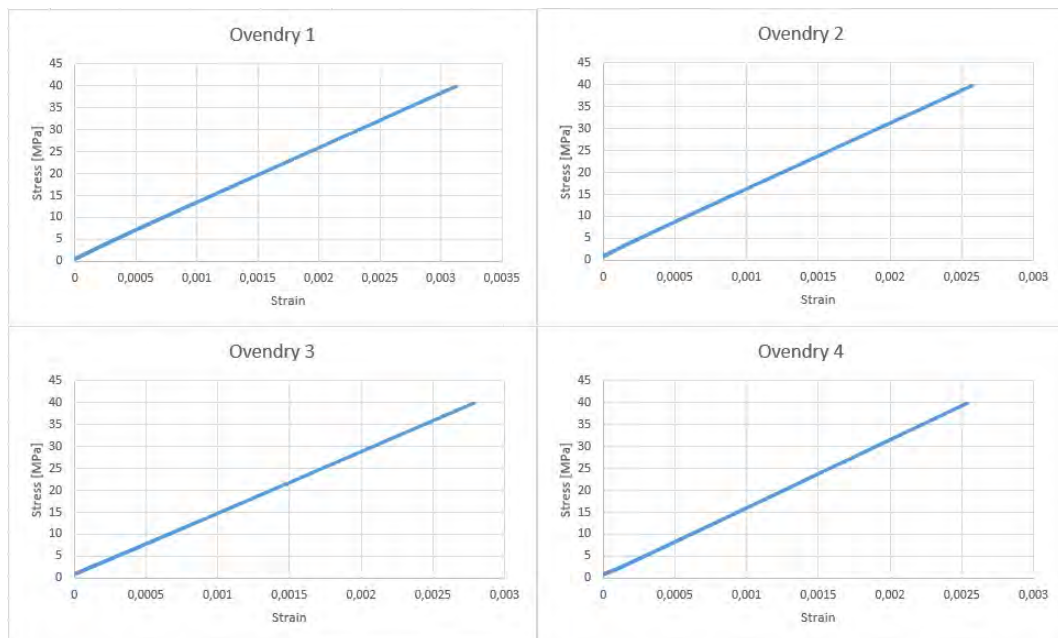


Figure C.2: Strain measured of ovendry samples at 25 °C

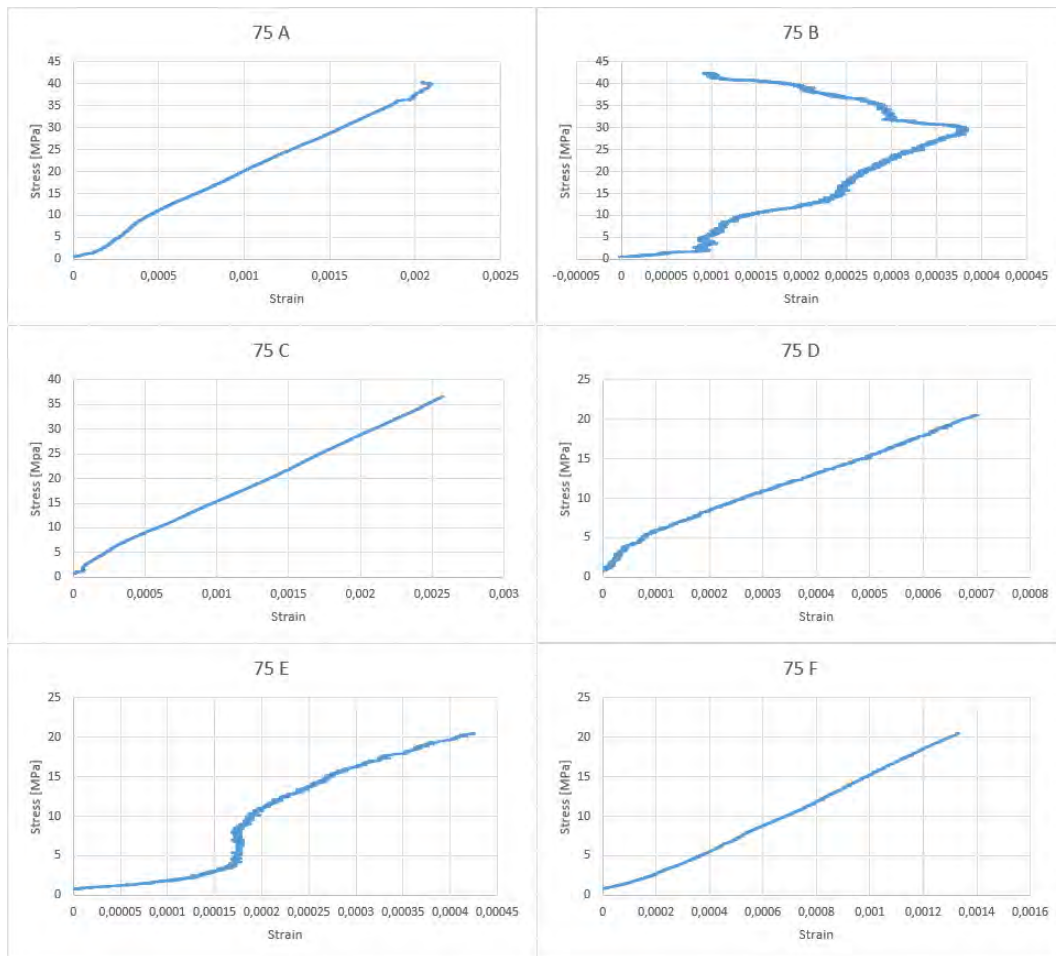


Figure C.3: Strain measured of samples at 75 °C

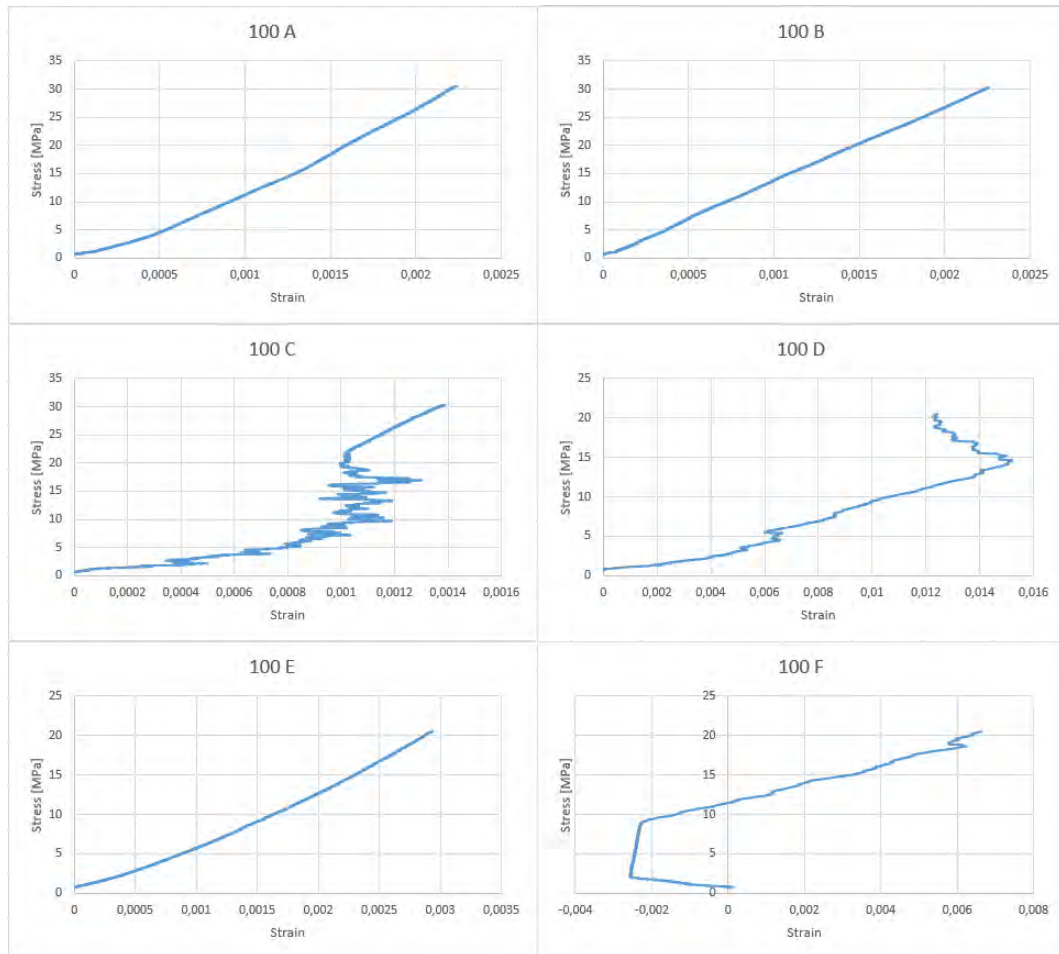


Figure C.4: Strain measured of samples at 100 °C

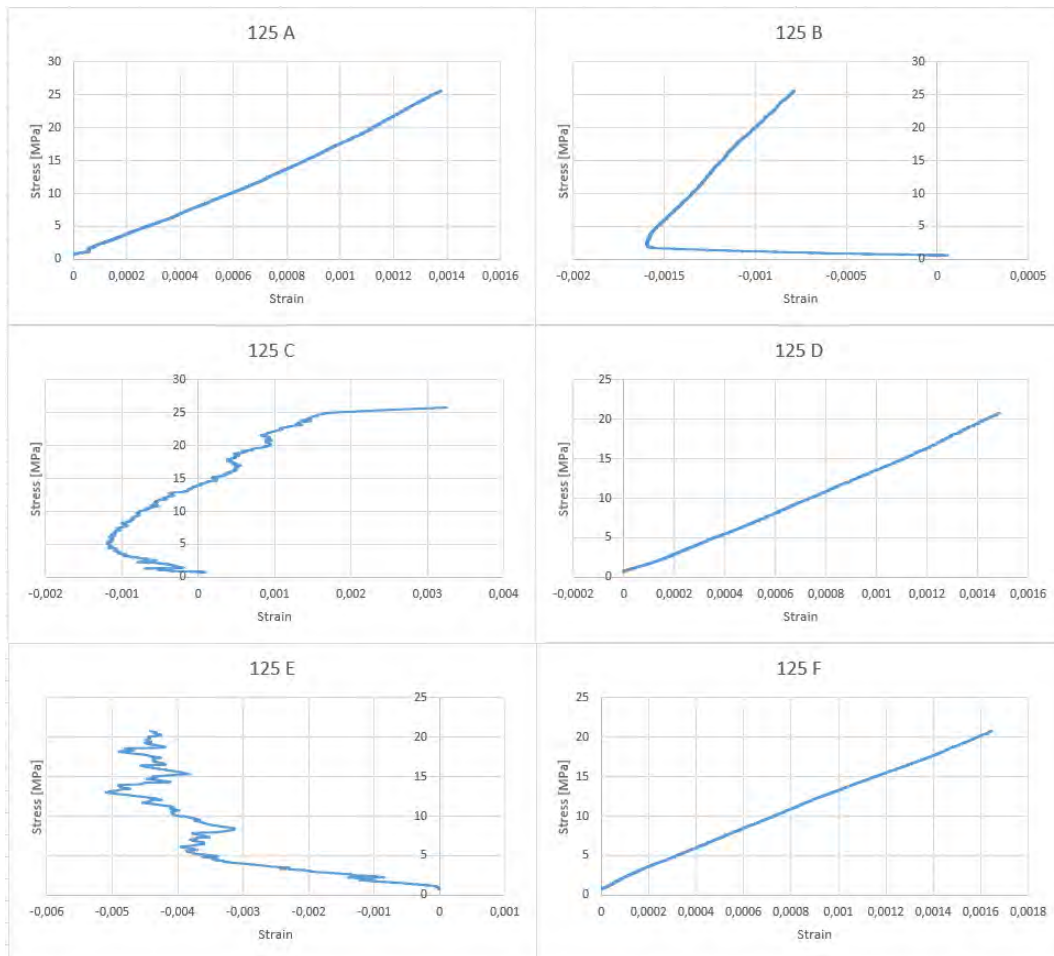


Figure C.5: Strain measured of samples at 125 °C

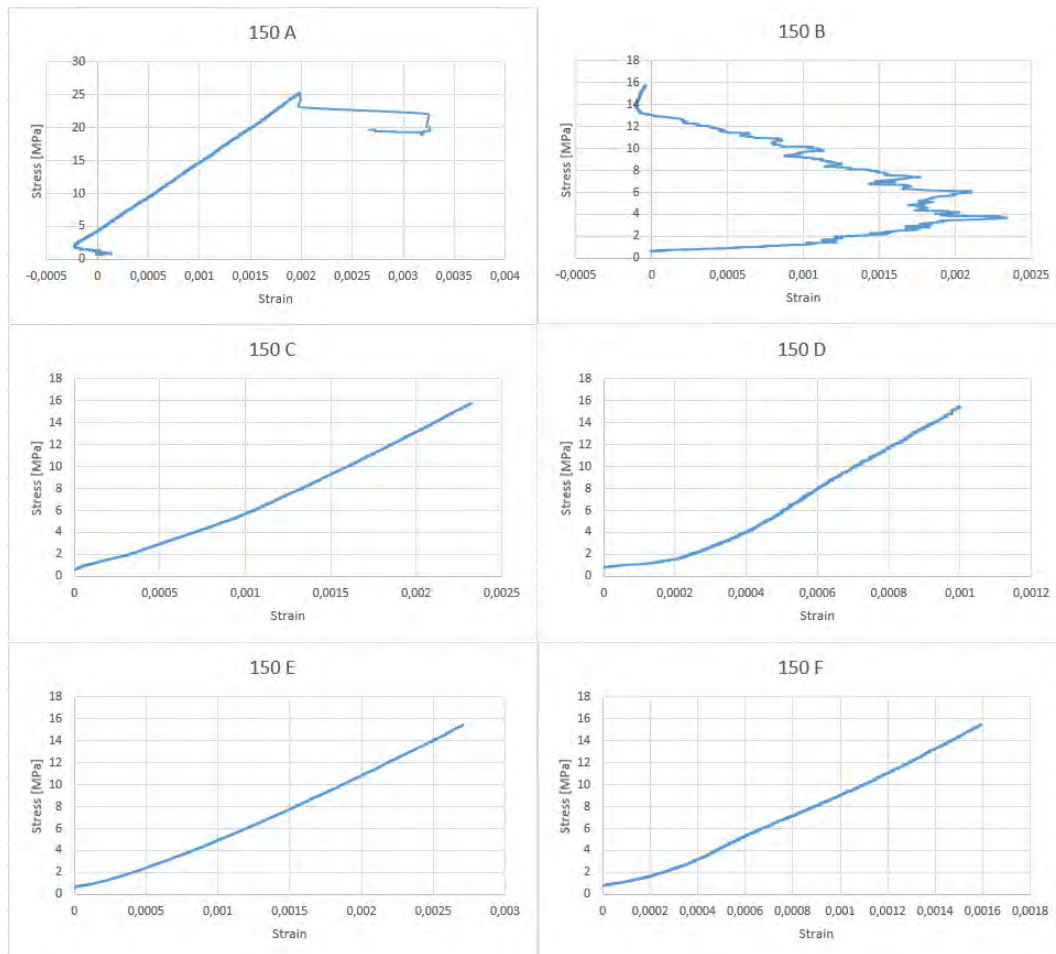


Figure C.6: Strain measured of samples at 150 °C

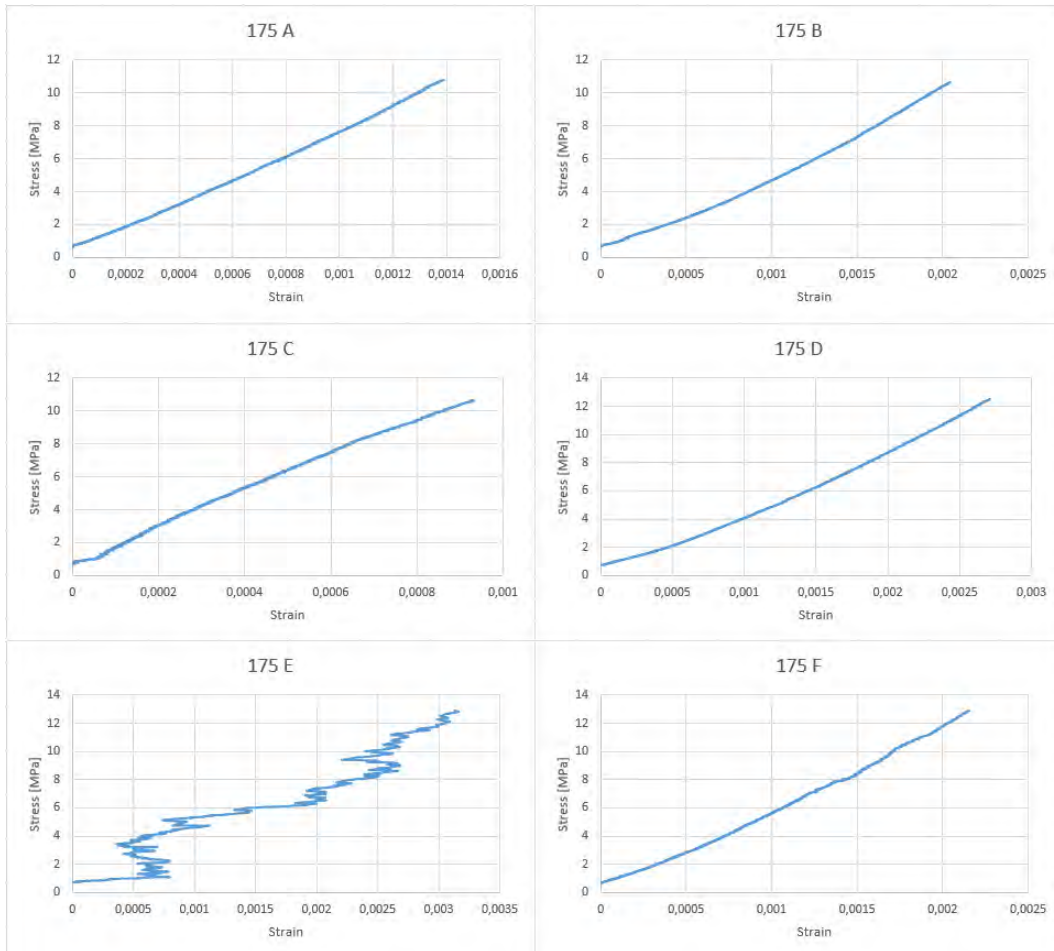


Figure C.7: Strain measured of samples at 175 °C

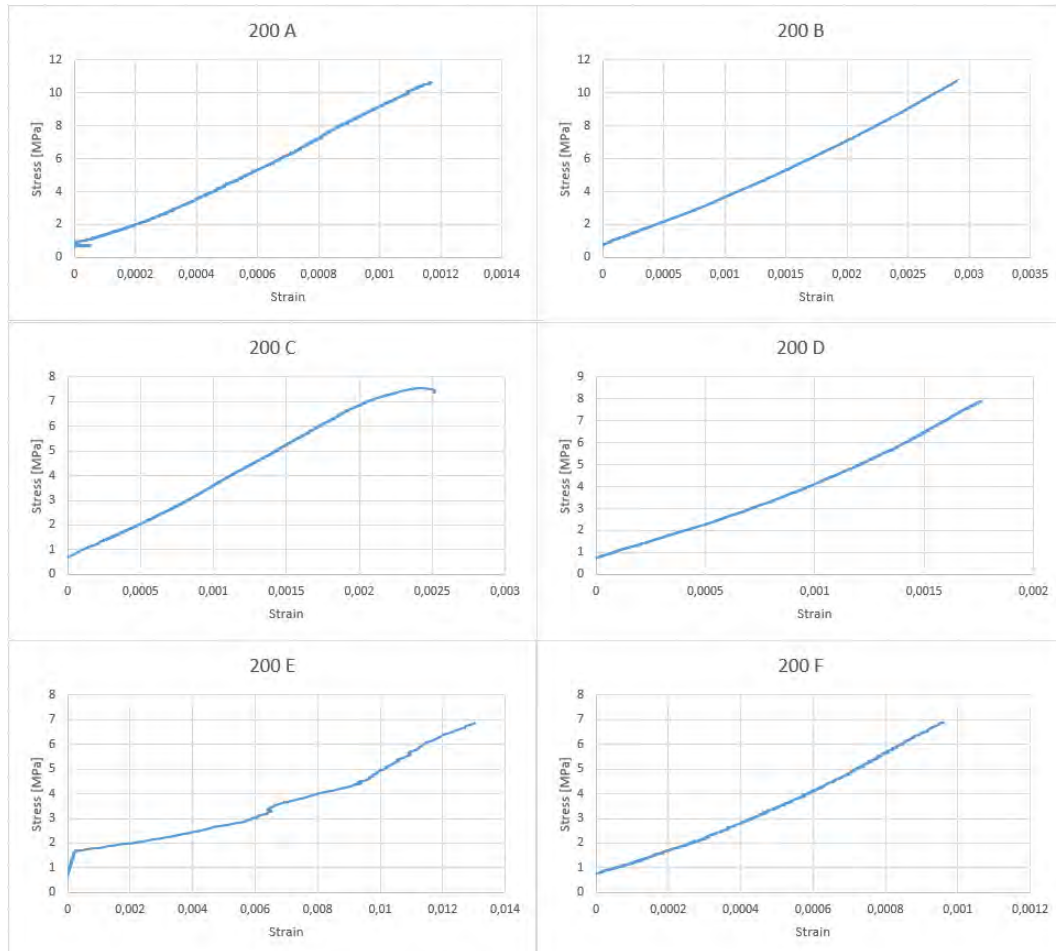


Figure C.8: Strain measured of samples at 200 °C

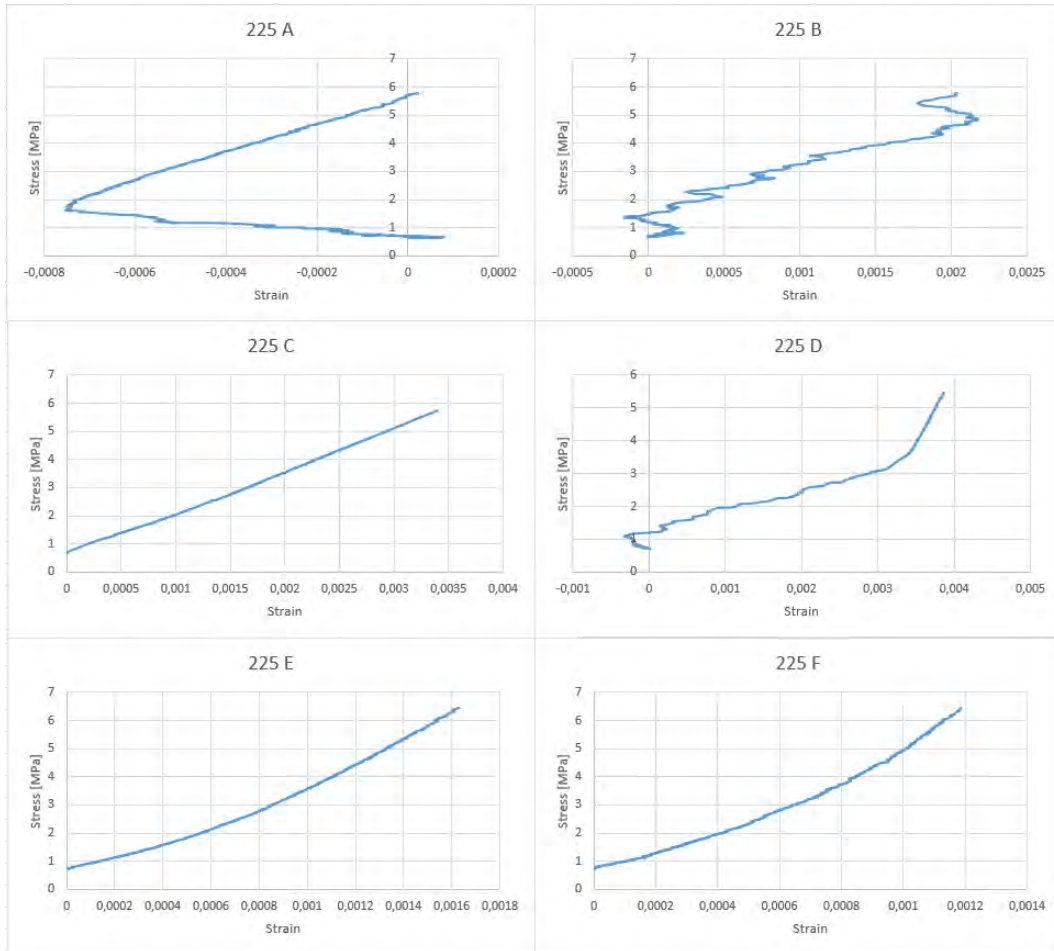


Figure C.9: Strain measured of samples at 225 °C

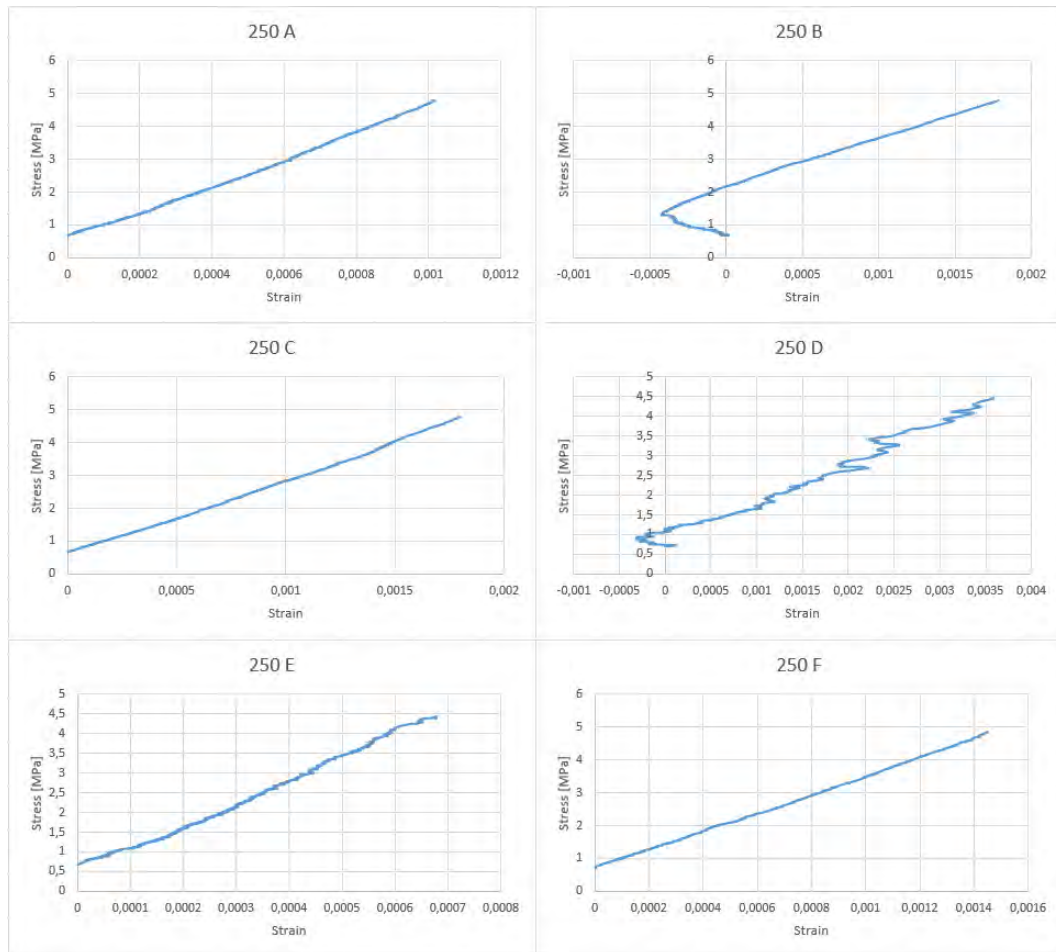


Figure C.10: Strain measured of samples at 250 °C

Appendix D

Breakage of specimen



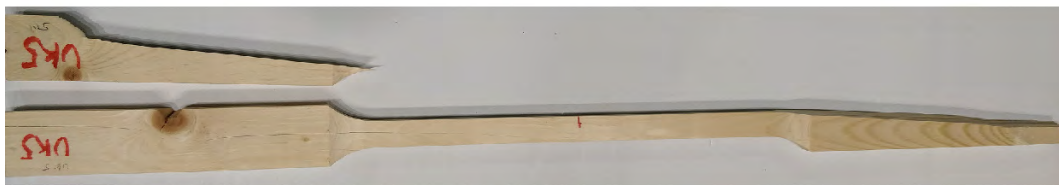
Ovendry 1



Ovendry 2



Ovendry 3



Ovendry 4

Figure D.1: Breakage of ovendry samples at 25 °C



75 A



75 B



75 C



75 D



75 E



75 F

Figure D.2: Breakage of samples at 75 °C



100 A



100 B



100 C



100 D



100 E



100 F

Figure D.3: Breakage of samples at 100 °C



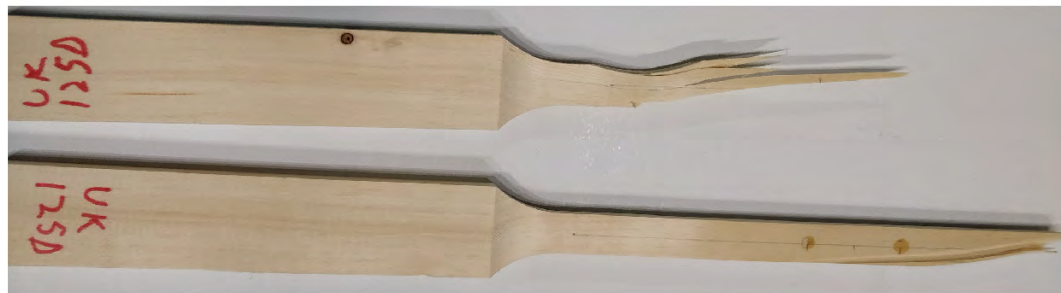
125 A



125 B



125 C



125 D



125 E



125 F

Figure D.4: Breakage of samples at 125 °C

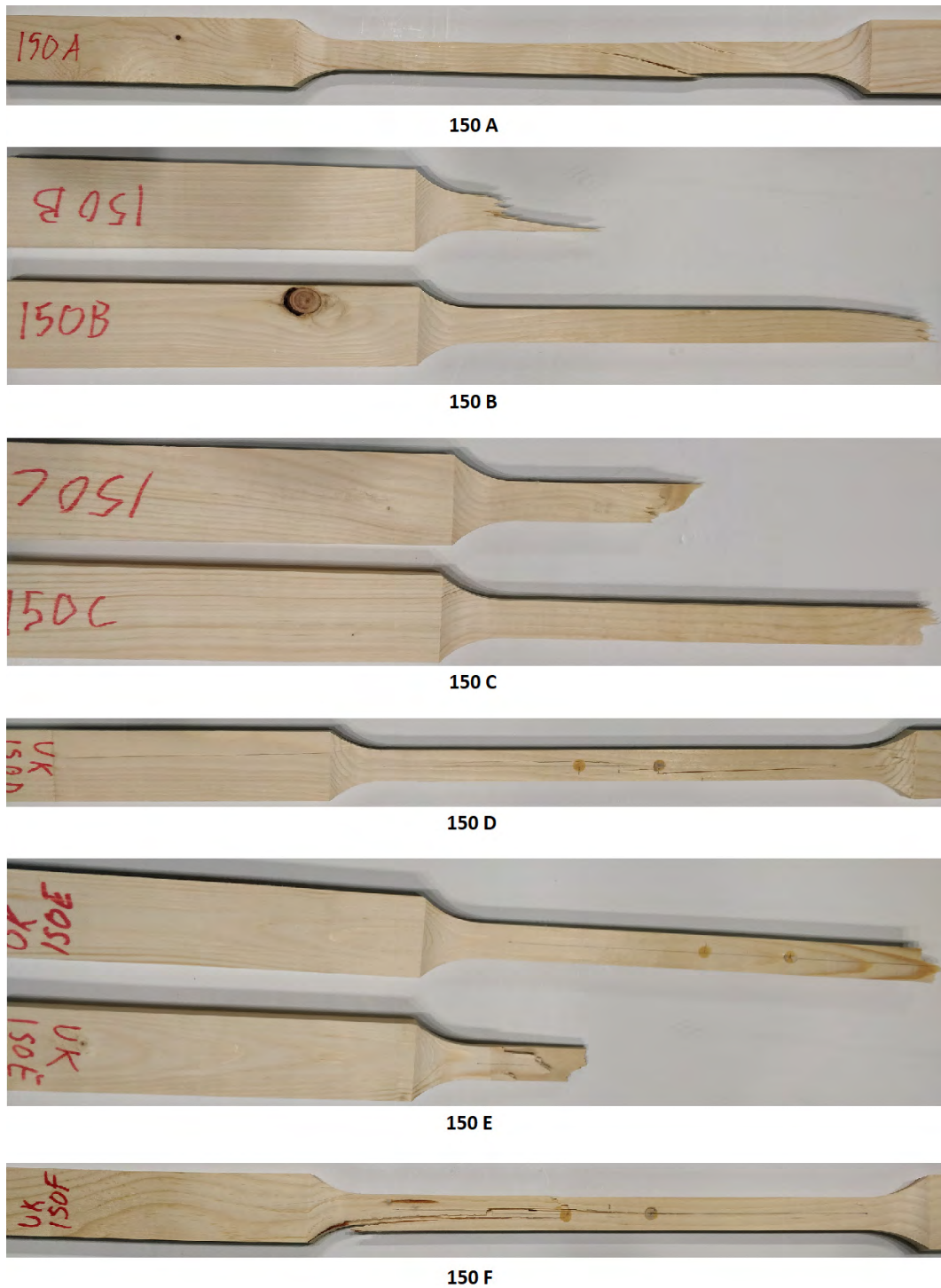


Figure D.5: Breakage of samples at 150 °C



Figure D.6: Breakage of samples at 175 °C



Figure D.7: Breakage of samples at 200 °C



225 A



225 B



225 C



225 D



225 E



225 F

Figure D.8: Breakage of samples at 225 °C



Figure D.9: Breakage of samples at 250 °C